The Journal of Toxicological Sciences (J. Toxicol. Sci.)
Vol.33, No.1, 37-50, 2008

Original Article

Gene expression profiling of methapyrilene-induced hepatotoxicity in rat

Takeki Uehara[1], Naoki Kiyosawa[1], Mitsuhiro Hirode[1], Ko Omura[1], Toshinobu Shimizu[1], Atsushi Ono[1], Yumiko Mizukawa[1,2], Toshikazu Miyagishima[1], Taku Nagao[3] and Tetsuro Urushidani[1,2]

[1]Toxicogenomics Project, National Institute of Biomedical Innovation, 7-6-8 Saito-Asagi, Ibaraki, Osaka 567-0085, Japan

[2]Department of Pathophysiology, Faculty of Pharmaceutical Sciences, Doshisha Women's College of Liberal Arts, Kodo, Kyotanabe, Kyoto 610-0395, Japan
[3]National Institute of Health Sciences, 1-18-1 Kamiyoga, Setagaya-ku, Tokyo 158-8501, Japan

(Received October 18, 2007; Accepted October 26, 2007)

ABSTRACT — The present study was conducted as a model case of the toxicogenomics approach for analyzing toxicological mechanisms and toxicity assessments in the early stage of drug development by comparing with classical toxicology data. Methapyrilene (MP) 100 mg/kg produced obvious histopathological changes in liver of rats by single or repeated dose up to 28 days with significant elevation of ALT and AST. In the middle dose groups (30 mg/kg MP), no apparent changes were noted in blood biochemical data by single dosing or repeated dosing up to one week, and no obvious histopathological changes were observed except a slight hypertrophy in the hepatocytes. Comprehensive gene expression changes were analyzed using Affymetrix GeneChip® and differentially expressed probe sets were statistically extracted. These contained many genes related to "glutathione metabolism", "apoptosis", "MAPK signaling pathway" and "regulation of cell cycle", which were all thought to be involved in the development of presently observed phenotypes. In the high dose groups, TGP1 scores (developed in our system in order to overview the responsiveness of drugs to multiple marker gene lists) for these categories were markedly increased from the early time point after single dose and kept their high expression throughout the repeated dose period. In the middle dose groups, the increment of the scores were noted not only at the time points when apparent pathological changes emerged, but also at the earlier stage of repeated dosing and even after single dosing. We conclude that toxicogenomics would enable a more sensitive assessment at the earlier time point than classical toxicology evaluation.

Key words: Methapyrilene; Rat; Liver; Toxicogenomics; Microarray

INTRODUCTION

The toxicogenomics approach has attracted attention in the field of drug safety assessment as a promising tool in predicting the toxicity of chemicals and analyzing the mechanism of toxicity. Classical toxicology works to characterize the emerged toxic changes, but it is not always powerful in predicting potential toxicity that has not emerged at the point of assessment but might occur in the future or to detect serious disease without apparent change in observation of the classical phenotype. On the other hand, extraction of toxicologically meaningful information from comprehensive gene expression analysis is expected to be useful since these changes precede toxicity and occur in the lower dose range.

The toxicogenomics project was a 5-year collaborative project conducted by the National Institute of Health Sciences, the National Institute of Biomedical Innovation and 15 pharmaceutical companies in Japan that started in 2002 (Urushidani and Nagao, 2005). Its aim was to construct a

Correspondence: Tetsuro Urushidani (E-mail: turushid@dwc.doshisha.ac.jp)

large-scale toxicology database of transcriptome for prediction of toxicity of new chemical entities in the early stage of drug development. About 150 chemicals, mainly medicinal compounds, were selected, and gene expression in the liver (also the kidney in some cases) was comprehensively analyzed by Affymetrix GeneChip®. In 2007, the project was finished and the whole system, consisting of the database, the analyzing system and prediction system, was completed and named as TG-GATEs (Genomics Assisted Toxicity Evaluation System developed by the Toxicogenomics Project, Japan).

In the present study, we selected methapyrilene, a prototypic hepatotoxicant (Lijinsky *et al.*, 1980), as a model case of the toxicogenomics approach for analyzing the toxicological mechanism and toxicity assessment in the early stage of drug development by comparing with classical toxicology data.

MATERIALS AND METHODS

Chemical

Methapyrilene (MP) was obtained from Sigma Chemical Company (St. Louis, MO, USA) and a suspension formulation was prepared by mixing with 0.5% methylcellulose (MC) solution.

Animal and experimental design

Five-week old male Sprague-Dawley rats were obtained from Charles River Japan Inc. (Kanagawa, Japan). After a 7-day quarantine and acclimatization period, the animals (6-week old) were assigned to dosage groups (5 rats per group) using a computerized stratified random grouping method based on individual body weight. The animals were individually housed in stainless-steel cages in an animal room that was lighted for 12 hr (7:00–19:00) daily, ventilated with an air-exchange rate of 15 times per hour and maintained at 21–25°C with a relative humidity of 40–70%. Each animal was allowed free access to water and pellet diet (CRF-1, sterilized by radiation, Oriental Yeast Co., Tokyo, Japan).

According to the standard protocol in our project, rats received single or repeated doses of MP by gavage at doses of 0 (vehicle only), 10, 30 or 100 mg/kg. For the single-dose study, rats were sacrificed at 3, 6, 9 and 24 hr after dosing. For the repeated dose study, the animals were treated daily for 3, 7, 14 and 28 days, and they were sacrificed 24 hr after the last dosing. The animals were euthanized by exsanguination from the abdominal aorta under ether anesthesia after blood sampling, and liver samples were obtained from the left lateral lobe of the liver in each animal immediately after sacrifice for the following examinations.

The experimental protocols were reviewed and approved by the Ethics Review Committee for Animal Experimentation of the National Institute of Health Sciences.

Blood chemical examination

Blood samples were collected upon sacrifice in tubes containing heparin lithium, and aspartate aminotransferase (AST) and alanine aminotransferase (ALT) were measured using an auto analyzer (Hitachi 7080).

Histopathological examination

For light microscopic examination, liver samples were fixed in 10% neutral buffered formalin, dehydrated in alcohol and embedded in paraffin. Paraffin sections were prepared and stained by a routine method using hematoxylin and eosin (H&E).

Microarray gene expression analysis

Microarray analysis was conducted on 3 out of 5 samples for each group. Total RNA was isolated from RNAlater® (Ambion, Austin, TX, USA)-preserved samples using RNeasy kit by Bio Robot 3000 (Qiagen,Valencia, CA, USA). Homogenization was conducted by Mill Mixer (Qiagen) and zirconium beads. Purity of RNA was checked by gel electrophoresis confirming that the 260/280 nm ratio was between 2.2 and 3.0. Gene expression analysis was carried out using GeneGhip® RAE230A probe arrays (Affymetrix, Santa Clara, CA, USA) containing 15,923 probe sets. The procedure was basically conducted according to the manufacture's instructions as previously reported. Microarray Analysis Suite 5.0 (MAS; Affymetrix) was used to quantify microarray signals and the intensities were normalized for each chip by setting the mean intensity to 500 (per chip normalization).

Microarray data analysis

To determine differentially expressed genes between high and time-matched control sample groups, Welch's *t* test was applied with a p cut off value of 0.01 in combination with a 1.5-fold regulation-ratio of means using GeneSpring software (Agilent Technologies, Inc., Santa Clara, CA, USA). Probe sets, which were labeled as absent by Affymetrix detection call in any of the 48 samples in single or repeated dose study, were excluded from further analysis. For the extracted probe sets, showing significant changes for at least one time point of either single or repeated administrations, pathway and GO analysis was performed using David 2.1 beta (http://david.abcc.ncifcrf.gov/) to identify overrepresented gene categories in

each gene list, and a p value of < 0.05 determined by Fisher's exact test was considered statistically significant.

Scoring of the marker gene sets (TGP1 score)

To facilitate the analytical procedures for large-scale microarray data, we developed a simple one-dimensional score, named TGP1, which is useful to overview the trend of the changes in expression of multiple biomarker gene lists all at once (Kiyosawa *et al.*, 2006). For each gene list, the signal log ratio was calculated by dividing the mean signal value of the chemical-treated group by that of the corresponding control. First, the sum of the signal log ratios for the used probe sets was calculated, and then divided by the number of probe sets used (Index 1). Next, the sum of squared signal log ratios for the used probe sets was calculated, and then divided by the number of probe sets used (Index 2). Finally, the TGP1 score was calculated by multiplying Index 1 with Index 2.

Statistical analysis

For blood chemical parameters, ANOVA followed by Dunnett's multiple comparison test or Kruskal-Wallis mean rank test followed by Mann-Whitney's U test was used as appropriate (Snedecor and Cochran, 1989).

RESULTS

Conventional toxicological parameters

Measurements of AST and ALT, representative markers of hepatotoxicity, are shown in Fig. 1 and histopathological findings are summarized in Tables 1 and 2. In the highest dose groups, both AST and ALT were elevated 3 or 6 hr after treatment, and they kept increasing with time. They also showed histopathological changes at every time point, such as hepatocellular hypertrophy and single cell necrosis in the peripheral lobular region, and obvious inflammation and anisonucleosis were noted at 24 hr after dosing (Fig. 2a). Furthermore, these lesions were aggravated and additional regenerative changes such as increased mitosis, bile duct proliferation, and hyperplasia, during repeated administrations were evident (Fig. 2b). In the middle dose groups, no apparent changes were noted in blood biochemical data by single dosing or repeated dosing up to one week, and no obvious histopathological changes were observed except a slight hypertrophy in the hepatocytes. At the time of the 15th and 29th days, single cell necrosis and infiltration of mononuclear cells were noted as in the highest group, though their severity was low. In the lowest dose groups, no obvious changes were noted either in blood biochemistry or in histopathology except for one case with hepatocyte hypertrophy in each of the 8th and 15th days.

Gene expression changes

Using the highest dose group showing obvious hepatotoxicity in terms of both blood biochemistry and histopathology, we extracted genes that showed statistically significant changes at least once in any time point in single and repeated dose experiments. For single and repeated dosing, up-regulated probe sets were 399 and 2509, respectively, and down-regulated probe sets were 235 and 876, respectively, namely, expression changes occurred in many genes in repeated dosing where obvious pathophysiological changes emerged.

Extracted genes were categorized by pathway and GO analysis and the results are summarized in Tables 3 (up-regulated) and 4 (down-regulated). Among the genes up-regulated in single dose experiments, gene ontologies or pathways related to "regulation of cell cycle", "MAPK signaling pathway" and "glutathione metabolism" were still significantly up-regulated in repeated dosing. The genes related to "apoptosis" or "ribosome" were clearly up-regulated in repeated dosing, while they were not affected by single dosing.

In single dose experiments, the number of down-regulated genes was quite a few (Table 4). Significant suppression of gene expression by repeated administration was noted in various categories, including "starch and sucrose metabolism", "steroid metabolism", "complement activation" and "complement and coagulation cascades".

We considered the pathways and GO categories of "glutathione metabolism", "apoptosis", "MAPK signaling" and "regulation of cell cycle" as most important in the toxicological mechanisms of MP. In order to overview the effects of MP on these pathways, we calculated the TGP1-score for each (Table 5). Upon calculation of the score, redundant probe sets were unified based on their reliability and dose-dependency. It is obvious from Table 5 that the marker scores of these categories markedly increased in the early stage of single dosing of the highest dose and they kept increasing during repeated dosing. In case of middle dosing, an obvious increase of scores for glutathione metabolism and apoptosis was detected not only at the 15th and 29th days with obvious pathological changes but also at the 4th and 8th days of repeated dosing and 6 hr after single dosing. In the lowest dose groups, the only detectable change was a tendency of increment in the score of apoptosis at the 8th day.

Up-regulated genes involved in glutathione metabolism, apoptosis, MAPK signaling pathway, and regulation of cell cycle

The individual gene expression change (ratio to control) in each category was depicted as heatmap (Fig. 3 to 6) for "glutathione metabolism", "apoptosis", "MAPK signaling" and "regulation of cell cycle", respectively. In general, most of the genes were dose-dependently mobilized and characteristic changes were noticed in single and repeated dosing groups. As for genes involved in glutathione biosynthesis: glutamate cysteine ligase, modifier subunit (Gclm) and glutamate-cysteine ligase, catalytic subunit (Gclc) (Fig. 3); those involved in the regulation of apoptosis: v-akt murine thymoma viral oncogene homolog 1 (Akt1) and programmed cell death 6 interacting protein (Pdcd6ip) (Fig. 4), and those belonging to heat shock proteins: heat shock 70 kD protein 1A/1B (Hspa1a/1b) and heat shock protein 8 (Hspa8) (Fig. 5), these were markedly up-regulated in the early stage of single dose, whereas little or no changes were noted in repeated dosing. Excluding these genes, the extent of up-regulation increased with repeated administration in most of the genes. Especially, those involved in glutathione metabolism: glucose-6-phosphate dehydrogenase (G6pdx), glutathione *S*-transferase M4 (Gstm4) and glutathione *S*-transferase Yc2 subunit (Yc2) (Fig. 3), those involved in regulation of apoptosis: nucleolar protein 3 (Nol3), rhoB gene (Rhob) and tribbles homolog 3 (Drosophila) (Trib3) (Fig. 4), those belonging to MAPK signaling and known as cell cycle regulators: myelocytomatosis viral oncogene homolog (avian) (Myc),

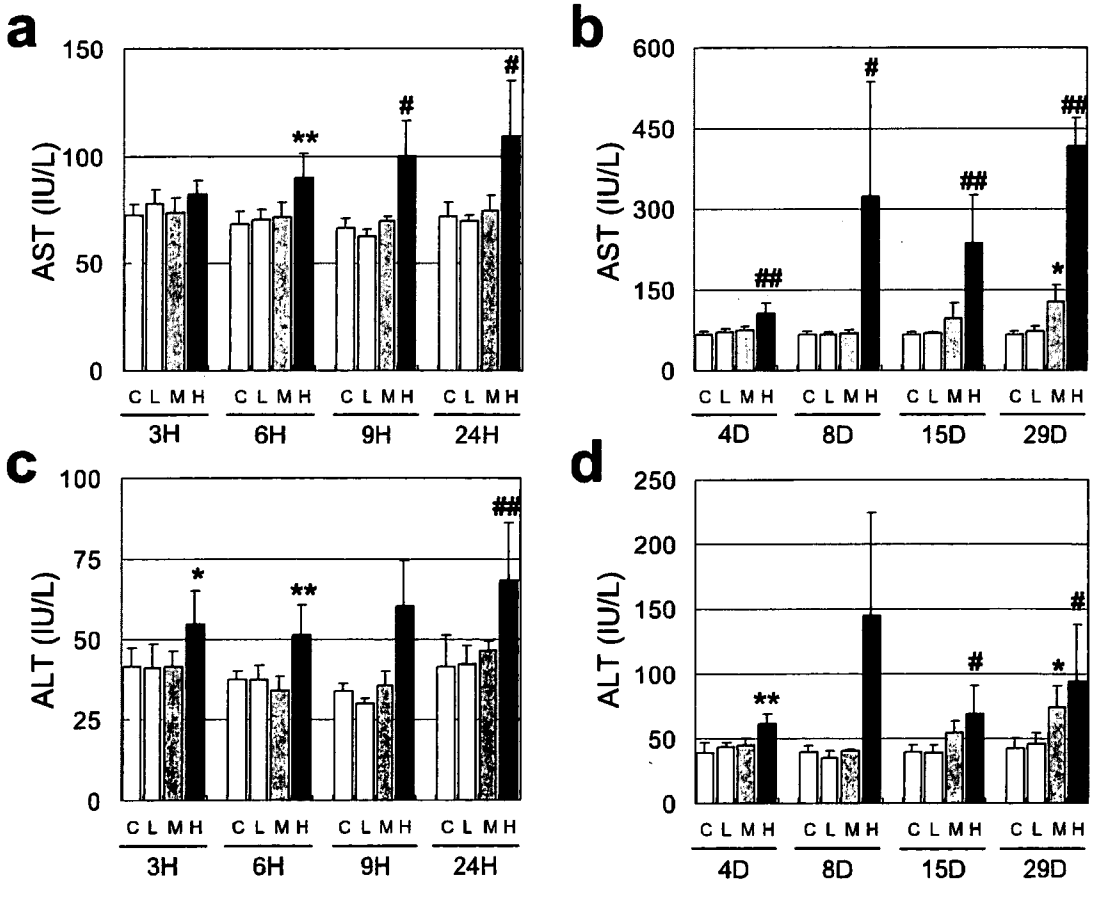

Fig. 1. Serum AST (a and b) and ALT activities (c and d) in rats treated with 10, 30 and 300 mg/kg MP in single and repeated dose studies.
Data are expressed as mean± S.D. (n = 5). *, **Significant difference from the control group, $p < 0.05$, 0.01, by Dunnett's multiple comparison test. #, ##Significant difference from the control group, $p < 0.05$, 0.01, by Mann-Whitney's U test.

Table 1. Histopathological findings in rat liver treated with MP in single dose study.

Morphology	Time Point (hrs)	3			6			9			24		
	Dose (mg/kg)	10	30	100	10	30	100	10	30	100	10	30	100
	Number of animals examined	5	5	5	5	5	5	5	5	5	5	5	5
Hepatocyte / Anisonucleosis		0	0	0	0	0	0	0	0	0	0	0	5
slight													5
Hepatocyte / Hypertrophy		0	0	1	0	0	3	0	0	4	0	1	5
slight				1			3			4		1	5
Hepatocyte / Single cell necrosis		0	0	1	0	0	3	0	0	5	0	0	5
slight				1			3			5			5
Periportal / Cellular infiltration, mononuclear cell		0	0	0	0	0	0	0	0	5	0	0	5
slight										5			5

Vehicle alone, or MP 10, 30, or 100 mg/kg was administered orally to rats, and the animals were euthanized at 3, 6, 9 and 24 hr after dosing (n = 5). The histopathological change in liver was graded into 4 categories: very slight, slight, moderate, and severe. The number of animals affected at each grade is shown.

Table 2. Histopathological findings in rat liver treated with MP in repeated dose study.

Morphology	Time Point (days)	4			8			15			29		
	Dose (mg/kg)	10	30	100	10	30	100	10	30	100	10	30	100
	Number of animals examined	5	5	5	5	5	5	5	5	5	5	5	4[a)]
Hepatocyte / Alteration, cytoplasmic		0	0	0	0	0	0		0	0	0	0	1
slight													1
Hepatocyte / Anisonucleosis		0	0	3	0	0	4		0	5	0	0	4
slight				3			4			5			4
Hepatocyte / Hyperplasia		0	0	0	0	0	0		0	0	0	0	4
slight													4
Hepatocyte / Hypertrophy		0	2	5	1	2	5		3	5	1	5	4
slight			2	5	1	2	5		3	5	1	5	4
Hepatocyte / Increased mitosis		0	1	4	0	0	3		1	0	0	3	3
slight			1	4			3		1			3	3
Hepatocyte / Single cell necrosis		0	0	5	0	0	5		3	5	0	3	4
slight				5			5		3	5		3	4
Interlobular / Proliferation, bile duct		0	0	5	0	0	5		1	5	0	0	4
slight				5			5		1	4			
moderate										1			4
Periportal / Cellular infiltration, mononuclear cell		0	1	4	0	0	4		5	5	0	2	4
slight			1	4			4		5	2		2	4
moderate										3			
Periportal / Deposit, pigment		0	0	0	0	0	0		0	0	0	0	3
slight													3

Vehicle alone, or MP 10, 30, or 100 mg/kg was administered orally to rats once daily for 1, 3, 7, 14, and 28 days, and the animals were euthanized at 24 hr after dosing, namely, on 2, 4, 8, 15, and 29 days (n = 5). [a)]One of the 5 rats died and was not examined histopathologically due to advanced autolysis. For more detailed information, see Table 1.

FBJ murine osteosarcoma viral oncogene homolog (Fos), v-jun sarcoma virus 17 oncogene homolog (avian) (Jun) and fibroblast growth factor 21 (Fgf21) (Fig. 5), and those related to DNA damage: growth arrest and DNA-damage-inducible 45 alpha (Gadd45a) and DNA-damage inducible transcript 3 (Ddit3) (Fig. 6), these kept up-regulated throughout the repeated dosing periods.

DISCUSSION

Methapyrilene hydrochloride is an antihistamine drug and had been used in the 1970s, but was removed from the market once it was known to be carcinogenic in rat liver (Lijinsky *et al.*, 1980; Fischer *et al.*, 1983). It is now considered to be a rat-specific carcinogen since hepatocellular carcinoma and cholangiocarcinoma were induced by administration of MP at 1000 ppm for 64 weeks, whereas no such findings were observed either in Syrian hamsters, Guinea-pigs, B6C3F1 mice, or humans (Mirsalis, 1987). As for its genotoxicity, the Ames test, DNA addition test, chromosome abnormality test (NTP, 2000) and irregular DNA synthesis test in rat and mouse (Steinmetz *et al.*, 1988) were all negative, whereas the cell transformation assay and L5178Y/TK+/– mouse lymphoma assay were positive (Turner *et al.*, 1987). Based on these observations, hepatocarcinogenicity of MP in rat has been considered to be non-genotoxic, whereas the involvement of its initiation activity cannot be completely excluded (Althaus *et al.*,

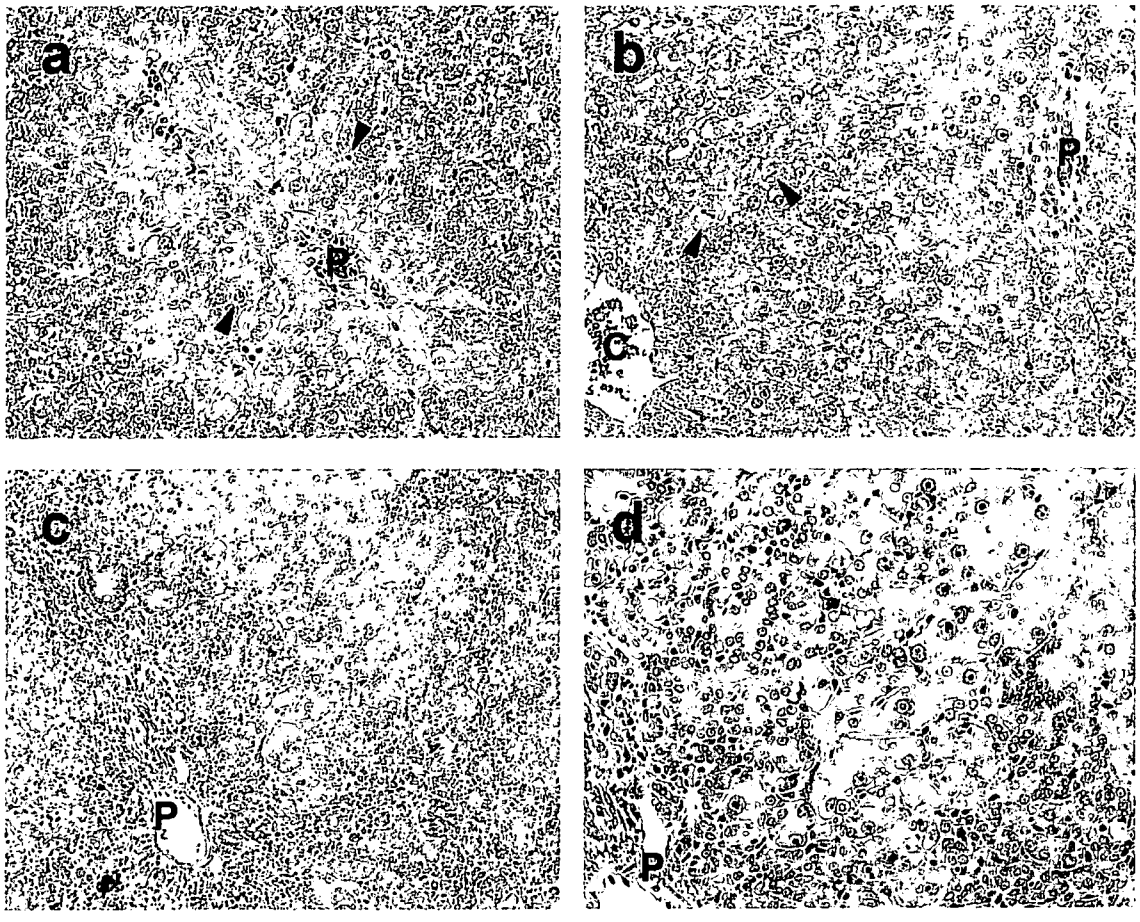

Fig. 2. Histopathological changes of liver treated with 100 mg/kg MP.
a: Hepatocellular hypertrophy and single cell necrosis (arrow head) in the periportal region (P) are observed at early time point, 24 hr after single dosing. b: Additional regenerative changes, such as increased mitosis, bile duct proliferation, and hyperplasia are evident by repeated administration.

Table 3. Gene ontology and pathway classification of extracted probe sets (up-regulation).

Exp. type	TERM[a)]	Count[b)]	p value[c)]
Single dose study			
	GOTERM_BP_5		
	REGULATION OF NUCLEOBASE, NUCLEOSIDE, NUCLEOTIDE AND NUCLEIC ACID METABOLISM	18	6.41E-2
	TRANSCRIPTION	18	7.48E-2
	MACROMOLECULE BIOSYNTHESIS	**13**	**1.92E-2**
	PROTEIN BIOSYNTHESIS	**11**	**3.84E-2**
	REGULATION OF CELL CYCLE	**11**	**5.95E-4**
	INTRACELLULAR TRANSPORT	**9**	**8.5E-2**
	AMINO ACID METABOLISM	6	2.75E-2
	AMINE BIOSYNTHESIS	5	9.11E-3
	CELL GROWTH	5	4.86E-2
	NUCLEAR TRANSPORT	5	2.6E-3
	NUCLEOCYTOPLASMIC TRANSPORT	5	6.12E-3
	PROTEIN KINASE CASCADE	5	4.18E-2
	REGULATION OF CELL SIZE	5	4.86E-2
	RNA METABOLISM	5	4.63E-2
	POSITIVE REGULATION OF NUCLEOBASE, NUCLEOSIDE, NUCLEOTIDE AND NUCLEIC ACID METABOLISM	4	8.74E-2
	PROTEIN IMPORT	4	1.49E-2
	RNA PROCESSING	4	6E-2
	GOTERM_CC_5		
	NUCLEUS	34	7.29E-3
	KEGG_PATHWAY		
	MAPK SIGNALING PATHWAY (Rattus norvegicus)	**10**	**3.73E-2**
	GAP JUNCTION (Rattus norvegicus)	6	5.15E-2
	TGF-BETA SIGNALING PATHWAY (Rattus norvegicus)	5	8.22E-2
	ARGININE AND PROLINE METABOLISM (Rattus norvegicus)	4	3.69E-2
	GLUTATHIONE METABOLISM (Rattus norvegicus)	**4**	**2.42E-2**
Repeated dose study			
	GOTERM_BP_5		
	CELLULAR PROTEIN METABOLISM	189	2.86E-8
	MACROMOLECULE BIOSYNTHESIS	**89**	**4.92E-17**
	PROTEIN BIOSYNTHESIS	**85**	**2.13E-19**
	INTRACELLULAR TRANSPORT	**60**	**1.22E-9**
	PROTEIN TRANSPORT	47	1.48E-6
	INTRACELLULAR PROTEIN TRANSPORT	44	4.84E-7
	APOPTOSIS	38	3.07E-4
	REGULATION OF CELL CYCLE	**32**	**6.48E-4**
	REGULATION OF APOPTOSIS	31	2.99E-4
	REGULATION OF PROGRAMMED CELL DEATH	31	3.48E-4
	GOTERM_CC_5		
	VESICLE-MEDIATED TRANSPORT	30	1.48E-2
	CYTOSKELETON	64	6.02E-2
	RIBOSOME	60	1E-13
	MICROTUBULE CYTOSKELETON	41	2.59E-3
	KEGG_PATHWAY		
	MICROTUBULE ASSOCIATED COMPLEX	29	6.25E-2
	CYTOSOLIC RIBOSOME (SENSU EUKARYOTA)	26	2.79E-11
	RIBOSOME (Rattus norvegicus)	40	1.79E-24
	FOCAL ADHESION (Rattus norvegicus)	36	6.68E-2
	MAPK SIGNALING PATHWAY (Rattus norvegicus)	**33**	**7.61E-2**
	TIGHT JUNCTION (Rattus norvegicus)	27	4.25E-3
	GLUTATHIONE METABOLISM (Rattus norvegicus)	**8[d)]**	**4.55E-2**

Pathway and GO analysis was performed using David 2.1 beta. Statistical significant terms are listed (Fisher's exact test, $p < 0.05$; threshold counts: greater than 10% of the number of probe sets involved in the examined gene list). Bold terms were commonly affected in both single and repeated dose studies. Shaded terms were further analyzed by scoring based on the TGP1-score.

Table 4. Gene ontology and pathway classification of extracted probe sets (up-regulation).

Exp. type	TERM[a)]	Count[b)]	p value[c)]
Single dose study			
	GOTERM_BP_5		
	REGULATION OF NUCLEOBASE, NUCLEOSIDE, NUCLEOTIDE AND NUCLEIC ACID METABOLISM	13	9.72E-2
	REGULATION OF TRANSCRIPTION	13	9.51E-2
	RESPONSE TO CHEMICAL SUBSTANCE	4	8.4E-2
	CHEMOTAXIS	3	5.47E-2
	STEROL METABOLISM	3	6.27E-2
	KEGG_PATHWAY		
	STARCH AND SUCROSE METABOLISM (Rattus norvegicus)	3	4.97E-2
Repeated dose study			
	GOTERM_BP_5		
	CARBOXYLIC ACID METABOLISM	45	2.26E-16
	ELECTRON TRANSPORT	37	2.19E-8
	CELLULAR LIPID METABOLISM	34	7.06E-8
	IMMUNE RESPONSE	27	5.94E-2
	RESPONSE TO PEST, PATHOGEN OR PARASITE	21	4.78E-5
	AMINO ACID METABOLISM	20	1.32E-7
	CELLULAR CARBOHYDRATE METABOLISM	18	1.36E-3
	LIPID BIOSYNTHESIS	15	2.41E-3
	STEROID METABOLISM	15	1.6E-5
	WOUND HEALING	14	4.27E-5
	BLOOD COAGULATION	13	2.03E-6
	FATTY ACID METABOLISM	13	2.59E-3
	MONOSACCHARIDE METABOLISM	13	3.96E-3
	AMINO ACID DERIVATIVE METABOLISM	12	2.04E-4
	COENZYME METABOLISM	12	1.31E-2
	COFACTOR BIOSYNTHESIS	11	1.7E-2
	COMPLEMENT ACTIVATION	11	1.28E-7
	HUMORAL IMMUNE RESPONSE	11	3.22E-6
	AMINE CATABOLISM	10	1.37E-5
	RESPONSE TO CHEMICAL SUBSTANCE	10	2.22E-2
	INFLAMMATORY RESPONSE	9	3.47E-2
	GOTERM_CC_5		
	MITOCHONDRION	38	2.07E-5
	ENDOPLASMIC RETICULUM	26	8.26E-6
	MICROSOME	18	5.64E-7
	KEGG_PATHWAY		
	TRYPTOPHAN METABOLISM (Rattus norvegicus)	22	5.32E-12
	COMPLEMENT AND COAGULATION CASCADES (Rattus norvegicus)	17	7.4E-7
	FATTY ACID METABOLISM (Rattus norvegicus)	17	3.65E-7
	GLYCINE, SERINE AND THREONINE METABOLISM (Rattus norvegicus)	11	5.69E-7
	BUTANOATE METABOLISM (Rattus norvegicus)	9	7.11E-4
	GAMMA-HEXACHLOROCYCLOHEXANE DEGRADATION (Rattus norvegicus)	9	1.29E-3
	LYSINE DEGRADATION (Rattus norvegicus)	9	1.26E-5
	PYRUVATE METABOLISM (Rattus norvegicus)	9	3.61E-4
	STARCH AND SUCROSE METABOLISM (Rattus norvegicus)	**9**	**1.08E-4**
	VALINE, LEUCINE AND ISOLEUCINE DEGRADATION (Rattus norvegicus)	9	3.61E-4

1982).

The analysis of hepatotoxicity of MP has been repeatedly performed by various techniques including the toxicogenomics approach (Hamadeh *et al.*, 2002). This compound induces marked and reproducible hepatic injury in rodents, and was used to assess the validity of toxicogenomics analyses among the multicenter platform (Waring *et al.*, 2004; Chu *et al.*, 2004). In the former study, there was a pessimistic interpretation that microarrays never supply highly reliable measures because of too large variance between research facilities. In this case, samples from the same animal were analyzed in multiple facilities but there were almost no genes that were detected as commonly changed in all the facilities. However, the latter study revealed that the robustness of the results regarding the movement of certain toxicological pathways was sufficient although the fitness of each gene was somewhat questionable. In other words, when we have a reasonable list of genes with certain toxicological significance, the reliability would be highly improved. The strategy of our project follows this idea, i.e., the results are interpreted as a trend for a set of functional genes.

Presently extracted genes from the group receiving the highest dose (showing obvious phenotypes) were categorized and this revealed that genes related to the regulation of cell cycle, MAPK signaling, and the glutathione metabolism were all involved in the development of the presently observed phenotypes. As for the down-regulated genes in repeated dosing, it could be a reflection of the failure of hepatic functions, *i.e.*, metabolism of sugar and sterols, and production of functional proteins such as complements and blood coagulation.

To facilitate the analytical procedures for our large-scale microarray database, we developed two types of the one-dimensional score, named as TGP1 and TGP2, which express the trend of the changes in expression of biomarker genes as a whole. The former is based on the signal log ratio (Kiyosawa *et al.*, 2006) and is convenient to compare the responsiveness of many drugs to a marker gene list. The disadvantages of this scoring system are that it overestimates the responsiveness when the list contains a gene where the induction is extreme (such as CYP1A1) and it

Table 5. Time course changes of TGP-1 scores in selected MP-responsive gene lists.

MP-RESPONSIVE GENE LISTS	03H			06H			09H			24H		
	L	M	H	L	M	H	L	M	H	L	M	H
GLUTATHIONE METABOLISM	23	2	7	2	39	607	−2	24	498	−35	−1	409
APOPTOSIS	6	7	103	3	24	342	8	10	128	0	2	195
MAPK SIGNALING PATHWAY	3	9	190	−2	7	114	−5	−26	15	−5	−2	57
REGULATION OF CELL CYCLE	3	2	108	−2	5	133	−3	−1	33	−3	−2	21
MP-RESPONSIVE GENE LISTS	04D			08D			15D			29D		
	L	M	H	L	M	H	L	M	H	L	M	H
GLUTATHIONE METABOLISM	2	118	476	2	170	3466	0	235	2285	5	712	2865
APOPTOSIS	2	54	286	93	227	1172	3	154	1360	−4	115	1396
MAPK SIGNALING PATHWAY	13	3	34	13	60	295	3	68	354	7	29	378
REGULATION OF CELL CYCLE	10	4	7	13	20	219	1	15	247	4	28	470

AFFYMETRIX PROBE ID	SYMBOL	03H			06H			09H			24H			04D			08D			15D			29D		
		L	M	H	L	M	H	L	M	H	L	M	H	L	M	H	L	M	H	L	M	H	L	M	H
1367856_at	G6pdx	1.1	0.9	0.9	1.2	1.4	2.5	1.1	1.5	4.2	1.0	1.4	2.9	1.4	0.8	1.4	0.6	0.9	1.8	1.1	1.2	3.9	1.0	0.8	5.0
1368374_a_at	Ggt1	1.1	1.0	0.9	1.1	0.9	0.7	1.0	0.7	0.9	1.0	1.2	1.3	1.0	1.0	1.3	1.3	1.4	2.8	1.1	1.3	4.5	0.9	1.3	8.0
1369081_at	Gsr	1.2	1.1	1.2	1.1	1.5	1.8	1.2	1.8	2.7	0.9	1.2	1.7	0.9	1.2	1.2	1.0	1.2	2.1	0.8	1.0	1.6	0.9	1.2	1.9
1369921_at	Gstm4	1.1	1.1	1.1	1.2	2.0	12	0.7	1.1	6.9	0.4	0.7	6.6	1.2	4.6	7.7	1.1	1.0	63	0.7	5.0	30	1.3	8.8	8.5
1369926_at	Gpx3	1.1	1.0	0.9	1.2	1.0	1.1	0.8	0.9	0.8	0.9	0.9	0.9	1.0	1.0	0.8	0.9	0.9	2.0	1.0	1.1	2.9	1.1	1.3	9.1
1370030_at	Gclm	1.1	1.2	1.3	1.2	1.4	2.5	1.2	1.8	2.1	0.9	0.7	1.0	1.1	1.3	1.0	1.1	1.0	1.6	1.0	1.2	1.3	0.9	0.8	1.0
1370365_at	Gss	1.4	1.1	1.2	1.0	1.3	1.2	0.9	1.0	1.2	1.1	1.1	2.1	0.9	1.1	1.6	0.7	0.9	2.0	1.0	1.1	2.7	1.0	1.2	2.4
1371089_at	Yc2	2.4	1.3	1.4	1.0	1.8	2.8	0.9	1.4	3.9	0.7	1.2	5.6	0.9	1.9	6.7	1.7	5.9	30	1.4	4.6	20	1.7	11	34
1372523_at	Gclc	1.4	1.4	1.7	1.4	2.4	3.6	1.4	2.2	3.8	1.0	0.9	1.4	0.9	1.2	1.3	1.0	1.1	1.1	1.0	1.1	1.0	0.9	1.0	1.0
1374070_at	Gpx2	1.3	0.9	1.0	1.2	1.0	1.8	0.7	0.6	1.5	0.9	1.0	1.3	1.4	1.2	2.0	1.4	1.1	3.7	1.2	1.3	3.4	1.3	1.6	13

The number in each column expresses the ratio to control (N=3).

Fig. 3. Heatmap of individual gene expression change in category of "glutathione metabolism".

also underestimates the responsiveness when the genes in the list are mobilized to either direction. To overcome these disadvantages, we employed another score, TGP2, based on the effect size. In the present study, we employed the TGP1 score for assessment of the responsiveness to the gene lists, *i.e.*, "regulation of cell cycle", "MAPK signaling" and "glutathione metabolism" since the direction of expression changes was uniform. In the highest dose group, the scores for these categories markedly increased from the early time point after single dose and kept their high expression throughout the repeated dose period. In the middle dose groups, the increment of the scores were noted not only at the time points when apparent pathological changes emerged, but also at the earlier stage of repeated dosing and even after single dosing. This indicates that the toxicogenomics approach enables more sensitive assessment at the earlier time point than classical toxicology evaluation. Among the responding genes, glutathione-related: glucose-6-phosphate dehydrogenase (G6pdx), glutathione *S*-transferase M4 (Gstm4) and glutathione *S*-transferase Yc2 subunit (Yc2), apoptosis related: nucleolar protein 3 (Nol3), rhoB gene (Rhob) and tribbles homolog 3 (Drosophila) (Trib3), MAPK signaling-related: myelocytomatosis viral oncogene homolog (avian) (Myc), FBJ murine osteosarcoma viral oncogene homolog (Fos), v-jun sarcoma virus 17 oncogene homolog (avian) (Jun) and fibroblast growth factor 21 (Fgf21), and DNA damage-related: growth arrest and DNA-damage-inducible 45 alpha (Gadd45a) and DNA-damage inducible transcript 3 (Ddit3), these were markedly up-regulated from the early point of dosing. Especially, Trib3, which showed typical changes in the present study, would be one

AFFYMETRIX PROBE ID	SYMBOL	03H			06H			09H			24H			04D			08D			15D			29D		
		L	M	H	L	M	H	L	M	H	L	M	H	L	M	H	L	M	H	L	M	H	L	M	H
1367827_at	Ppp2cb	1.1	1.0	1.0	0.9	0.9	1.0	1.1	1.0	1.0	0.9	0.9	1.1	0.9	1.0	1.1	1.0	1.1	1.8	0.9	1.2	2.1	1.0	1.2	2.2
1367831_at	Tp53	1.1	1.2	1.2	0.9	0.8	1.0	1.0	0.9	0.9	0.9	1.0	1.1	1.3	1.0	1.3	1.3	1.3	2.0	1.3	1.0	2.4	0.8	1.2	2.0
1367856_at	G6pdx	0.9	1.2	4.8	1.1	1.6	13	1.3	1.5	2.8	1.0	1.0	1.1	1.4	0.8	1.4	0.6	0.9	1.8	1.1	1.2	3.9	1.0	0.8	5.0
1367890_at	Casp2	1.0	0.8	0.8	1.0	0.8	0.9	0.9	1.1	0.8	0.9	1.0	1.1	1.1	1.0	1.0	1.1	1.2	1.3	0.9	1.0	1.2	1.1	1.1	1.9
1367922_at	Adam17	1.0	1.1	0.9	1.0	1.1	1.5	1.1	1.2	1.8	1.0	1.0	1.1	1.1	0.9	1.0	1.1	1.1	1.0	1.1	0.9	1.1	1.1	1.1	1.7
1368118_at	Bcl10	0.9	0.9	1.0	1.0	0.9	0.8	1.0	0.8	0.9	0.9	1.1	1.1	1.1	0.9	1.0	0.9	0.9	1.6	0.9	1.0	1.6	1.1	1.3	1.8
1368305_at	Casp8	1.1	1.0	1.0	0.7	0.9	0.8	0.8	0.8	0.9	0.9	0.9	1.0	1.3	1.0	1.4	1.0	0.9	1.1	1.0	1.1	1.1	0.9	1.1	1.8
1368544_a_at	Nol3	1.2	1.8	3.1	2.2	3.2	13	1.2	1.0	2.5	2.2	1.5	4.3	1.4	1.4	1.4	1.5	1.0	2.9	1.3	1.5	7.5	0.6	2.5	10
1368856_at	Jak2	1.1	1.1	1.0	1.1	0.9	1.1	1.0	1.1	1.1	1.3	1.2	1.3	1.3	1.0	1.1	1.0	1.1	1.6	1.0	0.8	2.4	0.9	1.1	3.9
1368862_at	Akt1	0.6	0.7	0.9	0.8	1.4	1.6	1.9	3.7	4.5	1.1	1.2	1.4	0.9	0.8	0.9	1.0	0.9	1.3	1.0	1.0	1.6	0.8	1.0	1.4
1368888_a_at	Rtn4	1.1	1.0	1.1	0.9	1.2	1.9	1.1	1.3	1.9	1.1	0.9	1.1	1.3	0.9	1.0	0.9	1.8	2.5	1.3	1.8	2.7	0.8	1.7	4.2
1369104_at	Prkaa1	1.2	1.3	1.8	0.9	1.3	2.6	1.4	1.2	1.3	1.0	0.7	1.0	0.9	1.1	1.3	0.7	0.8	1.6	0.9	1.4	2.1	1.0	1.5	2.0
1369122_at	Bax	1.1	1.1	1.1	0.9	1.1	1.1	1.0	0.9	1.1	1.0	1.0	1.2	1.0	0.9	1.2	1.2	1.4	3.7	0.8	1.1	3.3	0.8	1.6	4.3
1369948_at	Ngfrap1	1.0	1.0	1.0	1.0	1.0	1.0	1.0	0.9	1.3	0.9	1.0	1.4	1.3	1.7	1.7	0.7	1.1	12	1.5	1.7	37	0.9	4.5	63
1369958_at	Rhob	1.0	1.4	2.9	1.2	1.2	3.4	1.2	1.0	2.2	1.1	1.1	2.7	0.9	1.0	1.1	1.0	1.1	2.0	1.2	1.3	3.0	1.0	1.5	3.9
1369995_at	Faf1	0.9	0.9	0.9	1.0	1.0	1.0	1.0	1.1	1.1	1.1	0.9	1.1	1.0	1.0	1.0	1.0	1.0	1.3	0.9	0.9	1.2	1.0	1.0	1.6
1370080_at	Hmox1	0.8	0.9	1.0	1.0	1.0	1.2	1.0	0.8	0.8	1.1	0.8	1.3	1.2	1.0	1.0	1.1	1.1	1.7	1.2	1.4	2.1	0.9	1.1	2.5
1370113_at	Birc3	1.0	1.0	1.1	0.8	1.2	1.1	1.2	0.9	1.2	1.1	1.1	1.2	1.3	0.9	1.2	0.9	0.9	1.1	0.7	0.9	1.4	1.0	1.2	1.9
1370141_at	Mcl1	0.9	1.0	1.0	1.0	1.0	1.1	1.0	0.9	0.9	1.0	1.1	1.3	1.1	1.1	1.2	1.0	1.2	1.6	1.1	1.2	1.4	0.9	1.0	1.6
1370226_at	Cstb	0.9	1.0	1.7	1.0	1.0	3.9	1.2	1.1	1.9	0.8	0.7	0.9	1.2	1.0	1.1	0.9	1.2	1.4	1.0	1.2	2.0	1.0	1.1	2.4
1370243_a_at	Ptma	0.9	0.8	0.9	1.1	1.0	0.9	0.9	0.7	0.8	1.0	1.2	1.2	1.0	0.9	1.0	1.0	1.0	1.3	0.9	1.0	1.5	0.9	1.1	1.7
1370290_at	Tubb5	1.0	1.1	1.2	0.9	1.1	1.4	1.0	1.1	1.1	0.9	0.9	1.0	1.1	1.1	1.1	0.8	0.8	1.3	0.9	0.9	1.8	1.1	1.2	2.6
1370695_s_at	Trib3	0.9	1.1	0.9	1.2	1.5	3.7	1.1	1.2	3.1	1.3	1.5	1.9	1.0	6.5	27	9.8	21	137	1.1	13	77	2.6	8.0	40
1371672_at	App	1.1	0.9	0.9	1.2	1.4	2.5	1.1	1.5	4.2	1.0	1.4	2.9	1.1	1.0	1.4	1.1	1.4	5.0	1.1	1.7	8.0	1.0	2.3	8.9
1373733_at	Bok	0.9	0.9	0.9	0.9	1.0	1.1	1.1	1.2	1.2	0.9	1.0	1.4	1.2	1.0	1.1	1.2	1.0	1.1	1.0	1.0	2.2	1.0	1.1	3.5
1386866_at	Ywhag	1.1	1.0	1.1	1.0	1.0	1.1	1.1	1.0	1.1	1.0	1.0	1.2	1.0	1.0	1.2	1.1	1.2	1.7	1.0	1.1	1.8	1.0	1.2	2.2
1387021_at	Wig1	1.0	1.1	1.1	1.1	1.1	1.7	1.1	1.1	1.6	0.9	0.9	1.2	1.1	1.0	1.1	0.9	1.0	1.5	1.1	1.1	2.3	1.2	1.3	3.4
1387087_at	Cebpb	0.9	1.0	1.0	1.2	1.3	0.7	0.6	0.8	0.7	0.6	0.8	1.7	1.3	1.5	1.3	1.5	1.2	1.6	0.9	1.3	1.6	0.7	1.1	0.8
1387502_at	Stk17b	1.1	1.3	1.4	0.9	1.0	1.9	1.3	1.1	1.1	0.8	1.0	1.1	1.2	1.1	1.2	1.2	1.2	1.6	1.0	1.0	1.5	0.9	1.1	2.0
1387605_at	Casp12	1.0	1.1	1.0	0.9	1.0	1.4	1.1	0.9	1.2	0.9	0.6	1.0	1.3	1.0	1.6	1.2	1.1	1.7	1.8	2.6	5.3	0.4	0.9	1.6
1387618_at	Casp11	2.5	2.3	1.3	1.2	1.0	1.0	0.8	0.9	0.7	1.3	1.7	2.9	1.1	0.9	1.5	1.1	1.2	3.3	1.4	1.7	7.4	0.6	1.6	4.5
1388099_a_at	Tfpt	0.8	0.9	0.9	1.0	1.0	1.0	1.1	0.9	1.0	1.3	1.8	1.6	0.9	0.8	1.1	0.9	0.9	1.4	0.9	1.1	1.9	1.1	1.3	2.6
1388120_at	Pdcd6ip	0.7	2.0	8.0	0.9	3.9	14	2.7	2.9	8.5	1.4	0.6	16	1.0	1.0	1.2	0.9	1.0	1.3	1.0	1.0	1.5	0.9	1.0	1.6
1388674_at	Cdkn1a	1.0	1.1	1.0	0.9	1.0	1.0	0.9	1.0	1.5	1.0	1.3	2.0	1.1	1.0	1.5	0.9	1.5	2.1	1.2	1.8	2.1	0.8	1.9	1.7
1388805_at	Ppp2ca	0.9	0.8	0.9	0.9	1.0	1.1	0.9	0.9	1.1	0.9	1.1	1.1	1.2	1.1	1.5	0.9	1.0	1.7	0.8	1.0	2.7	1.1	1.3	3.6
1388867_at	MGC112830	0.9	1.1	1.2	1.2	1.3	1.7	1.0	1.2	1.6	0.8	0.8	1.0	1.0	1.1	1.1	0.9	1.1	1.3	1.0	1.0	1.2	0.9	1.0	1.7
1389170_at	Casp7	1.0	1.1	1.2	0.9	1.0	0.9	1.0	0.8	1.1	1.3	1.0	1.0	1.0	1.0	1.1	1.0	1.1	1.3	1.0	1.0	1.5	1.1	1.2	1.8
1398948_at	Tax1bp1	0.8	0.8	0.8	1.2	1.0	0.9	1.3	1.0	1.3	1.3	1.8	2.1	1.0	1.1	1.2	1.1	1.2	1.5	1.0	1.1	1.5	1.1	1.1	1.7

The number in each column expresses the ratio to control (N=3).

Fig. 4. Heatmap of individual gene expression change in category of "apoptosis".

of the promising candidates of biomarker genes for oxidative stress-mediated DNA damage, since it was reported to be up-regulated specifically by stress-inducing DNA damage (Corcoran *et al.*, 2005).

It was reported that hepatotoxicity of MP was due to its active metabolite(s) and that oxidative stress was involved (Ratra *et al.*, 1998). However, these authors excluded the involvement of glutathione depletion followed by oxidative stress in the later paper (Ratra *et al.*, 2000). We measured hepatic glutathione contents in rats treated with MP in a separate study (Uehara *et al.*, submitted). Immediately after MP dosing, a transient decrease, not statistically significant, was noted and a rebound-like increase was evident at 24 hr after dosing, which persisted for one week. The increment of glutathione contents disappeared till 2 weeks and it turned to a marked decrease after 4 weeks. These results suggest that MP causes oxidative stress in consuming glutathione while the hepatocytes defend against it by gene expression changes to keep a high glutathione level. Finally, glutathione depletion occurs when the toxicity of MP persists for a long period. We have extracted marker genes for hepatic glutathione depletion using a glutathione depletor, phorone (Kiyosawa *et al.*, 2007). Also in this work, phorone caused a transient decrease of glutathione with a peak at 3 to 6 hr after dosing followed by a rebound-like increase 24 hr after dosing. Taken together, the key of hepatotoxicity of MP is considered to be oxidative damage of DNA followed by changes in MAPK signaling and cell cycle induced by excess production of active metabolites. Sustained oxidative damage of DNA and stimulation of cell proliferation is closely related to hepatocarcinogenesis of MP.

The main purpose of the toxicogenomics approach was to analyze the mechanism of toxicity and predict chronic toxicity from acute data in the preclinical study. In the present study, we simulated the prediction of the toxicity

AFFYMETRIX PROBE ID	SYMBOL	03H			06H			09H			24H			04D			08D			15D			29D		
		L	M	H	L	M	H	L	M	H	L	M	H	L	M	H	L	M	H	L	M	H	L	M	H
1367577_at	Hspb1	1.0	0.9	0.6	1.3	1.4	1.4	0.6	0.8	1.0	1.2	1.3	2.0	1.2	1.5	1.1	1.4	1.3	2.9	0.9	1.3	3.1	0.9	1.6	2.9
1367624_at	Atf4	1.0	1.2	1.8	0.9	1.3	2.2	1.5	1.4	2.2	1.0	0.9	1.3	1.1	1.1	1.3	1.2	1.2	1.6	0.9	1.1	2.0	1.1	1.0	2.0
1367760_at	Map2k1	1.0	1.1	1.1	1.0	1.0	1.1	0.9	0.9	1.0	1.0	1.1	1.2	1.0	1.0	1.3	1.0	1.0	2.0	1.0	1.1	3.1	0.9	1.2	3.7
1367831_at	Tp53	1.0	0.9	0.9	1.0	1.0	1.0	1.0	1.1	1.3	1.1	1.3	1.2	1.3	1.0	1.3	1.3	1.3	2.0	1.3	1.0	2.4	0.8	1.2	2.0
1367890_at	Casp2	1.1	1.1	1.1	0.9	1.1	1.1	1.0	0.9	1.1	1.0	1.0	1.2	1.1	1.0	1.0	1.1	1.2	1.3	0.9	1.0	1.2	1.1	1.1	1.9
1368247_at	Hspa1a / 1b	0.9	1.2	1.4	1.4	1.4	2.8	1.1	1.1	1.5	1.5	1.7	1.8	1.2	1.1	1.8	1.5	1.5	1.4	0.8	1.2	1.2	0.7	0.6	0.4
1368273_at	Mapk6	1.1	1.2	1.2	1.0	1.3	1.8	1.0	1.1	1.4	1.1	1.0	1.0	0.9	0.9	0.9	0.9	0.9	1.1	1.0	0.9	1.1	0.9	1.0	1.0
1368277_at	Ppp3ca	1.1	0.9	1.0	0.9	0.9	1.2	1.2	1.2	1.2	1.1	1.1	1.2	1.0	1.1	1.1	1.0	1.3	1.3	1.1	1.0	1.3	1.2	1.1	1.6
1368305_at	Casp6	0.9	0.9	0.9	0.9	1.0	1.1	1.1	1.2	1.2	0.9	1.0	1.4	1.3	1.0	1.4	1.0	0.9	1.1	1.0	1.1	1.1	0.9	1.1	1.8
1368308_at	Myc	2.0	2.1	3.9	0.7	0.8	3.6	0.7	1.1	1.8	0.8	0.8	1.4	2.0	1.5	1.8	1.5	1.6	2.8	1.9	2.4	5.1	0.9	1.4	3.4
1368862_at	Akt1	1.0	0.8	0.8	1.0	0.8	0.9	0.9	1.1	0.8	0.9	1.0	1.1	0.9	0.8	0.9	1.0	0.9	1.3	1.0	1.0	1.6	0.8	1.0	1.4
1368871_at	Map3k1	1.3	1.0	1.0	0.8	0.7	0.7	0.8	1.2	1.2	0.8	0.7	0.7	0.9	0.9	0.8	0.9	1.0	2.0	1.0	1.2	2.4	1.1	1.0	3.0
1368947_at	Gadd45a	1.3	1.3	5.3	0.6	0.7	2.5	0.8	0.9	1.2	0.8	0.9	1.8	1.1	0.8	1.4	1.1	1.3	3.4	0.6	1.3	3.7	1.5	2.1	7.6
1369590_a_at	Ddit3	1.0	1.3	4.3	1.1	1.1	3.0	1.1	0.9	1.3	1.0	1.1	1.2	0.9	1.0	1.2	0.7	1.0	3.0	0.9	1.2	5.3	1.1	1.3	7.1
1369653_at	Tgfbr2	1.0	1.0	0.9	0.6	0.9	0.7	0.8	1.7	1.5	1.1	1.1	1.0	1.3	1.1	1.4	1.1	1.2	6.5	0.8	2.0	3.2	0.8	1.7	3.2
1369932_a_at	Raf1	1.0	1.1	1.1	1.0	1.2	1.6	1.2	1.2	1.6	0.9	0.9	1.0	1.0	1.1	1.0	0.9	0.9	1.1	1.0	0.9	1.2	0.9	0.9	1.2
1370035_at	Kras2	0.9	0.9	0.8	1.1	1.2	1.5	1.1	1.2	1.5	1.0	0.9	1.1	1.0	1.1	1.0	1.0	1.0	1.3	0.9	1.0	1.2	0.9	1.0	1.3
1370265_at	Arrb2	0.8	0.9	1.2	1.2	1.1	1.1	0.6	1.0	0.8	0.8	0.8	1.2	1.2	1.1	1.1	1.0	1.4	2.4	1.0	0.8	1.6	0.8	1.2	3.2
1370427_at	Pdgfa	0.9	0.8	0.9	1.5	2.4	4.2	1.0	0.9	2.0	0.8	0.7	1.2	1.2	1.1	1.1	2.6	2.5	5.4	0.8	2.0	4.5	0.9	1.0	4.1
1370585_a_at	Prkcb1	0.9	1.0	1.1	1.0	0.9	1.2	1.3	1.0	1.0	0.8	0.9	1.3	1.5	0.9	0.9	0.9	1.0	1.4	1.0	1.0	1.4	1.1	1.2	2.2
1370825_a_at	Cdc42	1.0	0.9	1.0	1.0	1.1	1.0	1.1	1.1	1.1	1.0	1.0	1.1	1.0	1.1	1.1	1.0	1.0	1.3	1.0	1.1	1.5	1.0	1.1	1.5
1370968_at	Nfkb1	1.0	0.9	1.0	1.0	1.0	1.2	1.0	1.0	1.2	1.0	0.8	1.1	1.1	0.9	1.0	1.0	1.0	1.3	1.2	1.1	1.9	1.0	1.2	2.0
1372982_at	Ppp3r1	0.9	1.3	1.3	1.1	1.3	1.5	1.4	1.2	1.2	0.9	1.0	1.2	1.0	1.1	1.0	0.9	0.9	1.5	0.9	0.7	1.1	1.1	1.2	2.2
1375043_at	Fos	0.4	0.3	3.6	0.5	1.0	3.4	2.8	1.7	3.0	0.2	0.2	0.2	0.8	0.8	0.6	1.5	5.5	14	0.5	1.0	6.8	1.8	1.7	15
1376425_at	Tgfb2	1.2	1.1	1.0	1.1	1.4	1.0	1.2	1.0	1.0	1.2	1.3	1.2	1.1	1.0	1.0	1.0	0.9	1.6	1.1	1.1	2.1	1.1	1.3	2.8
1386935_at	Nr4a1	1.1	1.0	1.4	1.1	1.0	1.5	0.7	0.8	0.8	1.1	1.0	1.0	1.2	1.0	1.0	0.9	0.9	1.4	1.0	1.0	1.5	1.1	1.5	2.7
1387377_a_at	Pak1	0.7	0.8	0.9	1.6	1.3	1.5	0.5	0.3	0.6	0.5	0.8	0.9	1.4	0.8	1.2	1.5	0.8	1.4	0.9	2.2	5.1	0.4	0.7	2.8
1387498_a_at	Fgfr1	1.0	0.8	1.0	0.7	0.9	0.7	0.9	1.0	0.9	1.0	1.0	0.9	1.0	1.1	0.9	1.5	1.4	1.9	1.0	1.0	1.3	0.8	1.0	2.3
1387643_at	Fgf21	1.2	2.1	8.8	0.6	1.2	3.6	0.7	1.0	1.6	1.0	1.1	5.1	1.1	1.5	3.9	1.1	5.0	7.5	0.9	4.8	6.4	3.1	3.5	6.6
1387771_a_at	Mapk3	1.2	1.2	1.1	1.1	1.0	0.9	0.9	1.1	0.9	1.1	0.9	1.0	1.2	1.2	1.0	0.9	1.1	1.2	0.9	0.9	1.3	0.9	0.9	2.1
1387806_at	Rap1b	1.0	1.0	1.0	1.0	1.0	1.2	1.0	1.0	1.1	0.9	0.9	1.1	1.1	1.0	1.0	1.0	1.1	1.3	1.0	1.0	1.4	1.0	1.1	1.6
1389170_at	Casp7	1.0	0.9	0.9	0.9	1.0	0.8	0.9	1.0	1.0	1.0	1.0	1.2	1.0	1.0	1.1	1.0	1.1	1.3	1.0	1.0	1.5	1.1	1.2	1.8
1389528_s_at	Jun	1.3	1.3	3.4	0.9	0.6	2.0	0.8	0.8	1.5	0.9	0.5	0.9	1.5	1.5	1.3	1.7	1.4	2.3	0.7	1.4	1.6	1.4	1.4	2.8
1398240_at	Hspa8	0.9	1.3	1.2	1.0	1.1	1.6	1.2	1.2	1.5	1.2	1.2	1.2	1.0	1.0	1.2	1.0	1.1	1.1	0.9	0.9	1.2	0.9	0.9	1.1
1398256_at	Il1b	0.7	0.6	0.6	0.8	0.6	0.8	0.9	0.9	1.1	0.5	0.7	1.1	2.3	0.8	1.5	1.2	1.1	1.5	1.0	1.1	1.8	1.2	1.0	2.1

The number in each column expresses the ratio to control (N=3).

Fig. 5. Heatmap of individual gene expression change in category of "MAPK signaling".

Gene expression in methapyrilene-treated rat liver.

AFFYMETRIX PROBE ID	SYMBOL	03H			06H			09H			24H			04D			08D			15D			29D		
		L	M	H	L	M	H	L	M	H	L	M	H	L	M	H	L	M	H	L	M	H	L	M	H
1367590_at	Ran	1.1	0.9	0.9	1.0	1.1	1.5	1.0	1.1	1.8	1.0	1.3	1.7	0.9	1.0	1.3	1.1	1.2	2.4	1.0	1.2	1.9	1.0	1.4	1.9
1367764_at	Ccng1	0.9	1.0	1.0	1.0	1.2	2.4	1.0	0.9	1.9	1.3	1.3	2.2	0.8	0.9	1.3	1.0	1.1	2.4	1.0	1.0	3.4	1.3	2.2	6.2
1367827_at	Ppp2cb	1.0	1.1	0.9	1.0	1.1	1.5	1.1	1.2	1.8	1.0	1.0	1.1	0.9	1.0	1.1	1.0	1.1	1.8	0.9	1.2	2.1	1.0	1.2	2.2
1367831_at	Tp53	1.0	0.9	0.9	1.0	1.0	1.0	1.0	1.1	1.3	1.1	1.3	1.2	1.3	1.0	1.3	1.3	1.3	2.0	1.3	1.0	2.4	0.8	1.2	2.0
1368076_at	Vhl	1.0	1.1	1.1	1.0	1.0	1.1	1.0	0.9	1.1	1.0	0.9	1.0	1.1	1.0	1.0	1.0	1.1	1.4	1.0	1.0	1.6	1.0	1.0	1.9
1368308_at	Myc	2.0	2.1	3.9	0.7	0.8	3.6	0.7	1.1	1.8	0.8	0.8	1.4	2.0	1.5	1.8	1.5	1.6	2.8	1.9	2.4	5.1	0.9	1.4	3.4
1368947_at	Gadd45a	1.3	1.3	5.3	0.6	0.7	2.5	0.8	0.9	1.2	0.8	0.9	1.8	1.1	0.8	1.4	1.1	1.3	3.4	0.6	1.3	3.7	1.5	2.1	7.6
1369590_a_at	Ddit3	1.0	1.3	4.3	1.1	1.1	3.0	1.1	0.9	1.3	1.0	1.1	1.2	0.9	1.0	1.2	0.7	1.0	3.0	0.9	1.2	5.3	1.1	1.3	7.1
1369932_a_at	Raf1	1.0	1.1	1.1	1.0	1.2	1.6	1.2	1.2	1.6	0.9	0.9	1.0	1.0	1.1	1.0	0.9	0.9	1.1	1.0	0.9	1.2	0.9	0.9	1.2
1369950_at	Cdk4	1.0	1.0	0.9	1.1	1.1	1.1	1.1	1.2	1.3	1.0	1.0	1.2	1.0	1.0	1.1	0.9	1.2	2.0	1.0	1.1	1.9	1.0	1.3	2.2
1369958_at	Rhob	0.9	1.0	1.7	1.0	1.0	3.9	1.2	1.1	1.9	0.8	0.7	0.9	0.9	1.0	1.1	1.0	1.1	2.0	1.2	1.3	3.0	1.0	1.5	3.9
1370035_at	Kras2	0.9	0.9	0.8	1.1	1.2	1.5	1.1	1.2	1.5	1.0	0.9	1.1	1.0	1.1	1.0	1.0	1.0	1.3	0.9	1.0	1.2	0.9	1.0	1.3
1370361_at	Cgref1	1.1	0.6	1.1	0.7	1.0	1.1	0.7	0.9	1.4	0.5	0.6	1.4	1.6	1.9	1.6	1.3	2.0	5.4	0.7	1.2	3.3	1.5	2.3	6.5
1370427_at	Pdgfa	0.9	0.8	0.9	1.5	2.4	4.2	1.0	0.9	2.0	0.8	0.7	1.2	1.2	1.1	1.1	2.6	2.5	5.4	0.8	2.0	4.5	0.9	1.0	4.1
1370504_a_at	Pmp22	1.2	1.5	1.2	0.8	0.9	1.1	0.7	0.7	0.6	0.8	0.8	1.0	1.2	1.4	1.3	1.3	1.6	1.6	1.1	1.3	1.5	1.8	1.4	2.7
1370809_at	Tubg1	1.1	1.0	0.9	1.0	1.0	1.1	1.0	0.9	1.0	1.0	1.0	1.4	1.1	1.2	1.1	1.1	1.0	1.5	0.9	1.2	2.2	1.2	1.5	2.6
1371308_at	Rps4x	1.0	1.0	1.0	0.9	1.0	1.0	1.0	1.0	1.1	1.0	1.1	1.2	1.0	1.0	1.1	1.0	1.1	1.6	1.1	1.3	1.6	1.2	1.3	1.6
1374956_at	Pcm1	1.2	0.9	1.1	0.9	0.9	0.9	1.3	1.1	1.2	1.0	1.1	1.0	1.0	0.9	0.9	1.2	1.2	1.4	1.0	0.9	1.3	1.1	0.9	1.6
1375630_at	RGD:1303103	1.0	0.8	1.0	1.0	1.1	1.3	1.1	1.0	1.4	1.0	1.1	1.3	0.9	1.0	1.0	1.2	1.2	1.6	1.1	1.2	1.9	1.0	1.2	1.8
1376425_at	Tgfb2	1.2	1.1	1.0	1.1	1.4	1.0	1.2	1.0	1.0	1.2	1.3	1.2	1.1	1.0	1.0	1.0	0.9	1.6	1.1	1.1	2.1	1.1	1.3	2.8
1379375_at	Pdgfa	1.1	1.1	1.1	1.0	1.2	2.0	0.9	0.9	1.6	0.7	0.8	1.1	1.2	1.1	1.3	0.8	1.0	1.9	0.9	0.9	2.1	1.1	1.3	3.0
1386866_at	Ywhag	1.1	1.0	1.1	0.9	1.2	1.9	1.1	1.3	1.9	1.1	0.9	1.1	1.0	1.0	1.2	1.1	1.2	1.7	1.0	1.1	1.8	1.0	1.2	2.2
1387391_at	Cdkn1a	0.9	1.1	0.9	1.1	1.5	3.9	0.6	0.7	2.8	1.2	2.2	2.9	1.2	1.1	1.4	1.9	2.5	5.9	1.1	2.1	3.1	0.9	2.8	2.5
1387616_at	Pdgfc	1.0	1.0	0.9	1.0	0.9	1.2	1.1	1.0	0.8	1.0	0.9	0.8	1.2	0.8	1.1	1.3	1.3	1.6	0.9	0.9	1.2	0.8	0.9	2.2
1387644_at	Btc	1.0	1.1	1.0	1.1	0.9	0.9	1.0	0.9	0.7	0.9	1.1	1.1	1.3	1.0	1.4	1.3	0.8	1.0	0.9	1.0	1.6	1.0	0.8	1.9
1387788_at	Junb	1.2	1.0	1.6	1.1	0.7	1.3	0.7	0.9	1.5	1.6	1.4	1.4	1.4	0.9	1.4	1.1	1.0	1.3	1.0	1.1	2.1	1.1	1.0	4.0
1388164_at	E2f6	1.0	1.0	1.1	1.0	1.4	1.7	1.0	1.1	1.7	1.2	1.1	1.2	1.0	1.0	1.1	1.1	1.1	1.4	1.0	1.0	1.5	0.9	1.1	1.7
1388805_at	Ppp2ca	1.1	1.0	1.0	1.1	1.0	1.4	1.1	1.0	1.4	0.9	1.0	1.5	1.2	1.1	1.5	0.9	1.0	1.7	0.8	1.0	2.7	1.1	1.3	3.6
1388867_at	MGC112830	1.0	1.1	1.2	0.9	1.1	1.4	1.0	1.1	1.1	0.9	0.9	1.0	1.0	1.1	1.1	0.9	1.1	1.3	1.0	1.0	1.2	0.9	1.0	1.7
1389101_at	Ccnc	0.7	0.7	0.5	0.9	1.1	1.2	1.2	1.0	0.8	1.2	1.1	1.4	1.2	1.1	1.1	1.1	1.3	2.0	1.3	1.6	2.5	1.5	1.6	2.5
1389528_s_at	Jun	1.3	1.3	3.4	0.9	0.6	2.0	0.8	0.8	1.5	0.9	0.5	0.9	1.5	1.5	1.3	1.7	1.4	2.3	0.7	1.4	1.6	1.4	1.4	2.8
1398240_at	Hspa8	0.9	1.3	1.2	1.0	1.1	1.6	1.2	1.2	1.5	1.2	1.2	1.2	1.0	1.0	1.2	1.0	1.1	1.1	0.9	0.9	1.2	0.9	0.9	1.1
1398256_at	Il1b	0.7	0.6	0.6	0.8	0.6	0.8	0.9	0.9	1.1	0.6	0.7	1.1	2.3	0.8	1.5	1.2	1.1	1.5	1.0	1.1	1.8	1.2	1.0	2.1

The number in each column expresses the ratio to control (N=3).

Fig. 6. Heatmap of individual gene expression change in category of "regulation of cell cycle".

of MP by focusing on the toxicological pathway drawn from transcriptome analysis. Genes up-regulated from the early stage described above would be promising candidates of biomarkers for hepatotoxicity. However, the present analysis focused on one chemical, MP. It is necessary to analyze other chemicals causing glutathione depletion/oxidative stress and nongenotoxic hepatocarcinogenesis, such as thioacetamide, coumarin and ethionine, in order to establish a useful and precise prediction system based on the toxicogenomics approach.

The greatest advantage of toxicogenomics in toxicology is that various toxicity mechanisms can be elucidated at once compared with the conventional strategy where many experiments are performed one by one. This strategy is so powerful that comprehensive seizure of what happens for the mechanism in the target organ is possible. Toxicogenomics enables one to supply supporting data for any conventional toxicological changes and suggests the appropriate toxicological mechanism behind them.

ACKNOWLEDGMENT

This work was supported in part by a grant from the Ministry of Health, Labour and Welfare (H14-Toxico-001).

REFERENCES

Althaus, F.R., Lawrence, S.D., Sattler, G.L. and Pitot, H.C. (1982): DNA damage induced by the antihistaminic drug methapyrilene hydrochloride. Mutat. Res., **103**, 213-218.

Chu, T.M., Deng, S., Wolfinger, R., Paules, R.S. and Hamadeh, H.K. (2004): Cross-site comparison of gene expression data reveals high similarity. Environ. Health Perspect., **112**, 449-455.

Corcoran, C.A., Luo, X., He, Q., Jiang, C., Huang, Y. and Sheikh, M.S. (2005): Genotoxic and endoplasmic reticulum stresses differentially regulate TRB3 expression. Cancer Biol. Ther., **4**, 1063-1067.

Fischer, G., Altmannsberger, M., Schauer, A. and Katz, N. (1983); Early stages of chemically induced liver carcinogenesis by oral administration of the antihistaminic methapyrilene hydrochloride. J. Cancer Res. Clin. Oncol., **106**, 53-57.

Hamadeh, H. K., Knight, B.L., Haugen, A.C., Sieber, S., Amin, R.P.,

Bushel, P.R., Stoll, R., Blanchard, K., Jayadev, S., Tennant, R.W., Cunningham, M.L., Afshari, C.A. and Paules, R.S. (2002): Methapyrilene toxicity: Anchorage of pathologic observations to gene expression alterations. Toxicol. Pathol., **30**, 470-482.

Kiyosawa, N., Shiwaku, K., Hirode, M., Omura, K., Uehara, T., Shimizu, T., Mizukawa, Y., Miyagishima, T., Ono, A., Nagao, T. and Urushidani, T. (2006): Utilization of a one-dimensional score for surveying the chemical-induced changes in expression levels of multiple biomarker gene sets using a large-scale toxicogenomics database. J. Toxicol. Sci., **31**, 433-448.

Kiyosawa, N., Uehara, T., Gao, W., Omura, K., Hirode, M., Shimizu, T., Mizukawa, Y., Ono, A., Miyagishima, T., Nagao, T. and Urushidani, T. (2007): Identification of glutathione depletion-responsive genes using phorone-treated rat liver. J.Toxicol. Sci., **32**, 469-486.

Lijinsky, W., Reuber, M.D. and Blackwell, B.N. (1980): Liver tumors induced in rats by oral administration of the antihistaminic methapyrilene hydrochloride. Science, **209**, 817-819.

Mirsalis, J.C. (1987): Genotoxicity, toxicity, and carcinogenicity of the antihistamine methapyrilene. Mutat. Res., **185**, 309-317.

NTP Hepatotoxicity Studies of the Liver Carcinogen Methapyrilene Hydrochloride (CAS No. 135-23-9) Administered in Feed to Male F344/N Rats. Toxic Rep Ser. 46:1-C7, 2000.

Ratra, G.S., Morgan, W.A., Mullervy, J., Powell, C.J. and Wright, M.C. (1998): Methapyrilene hepatotoxicity is associated with oxidative stress, mitochondrial disfunction and is prevented by the Ca^{2+} channel blocker verapamil. Toxicology, **130**, 79-93.

Ratra, G.S., Powell, C.J., Park, B.K., Maggs, J.L. and Cottrell, S. (2000): Methapyrilene hepatotoxicity is associated with increased hepatic glutathione, the formation of glucuronide conjugates, and enterohepatic recirculation. Chem. Biol. Interact., **129**, 279-295.

Snedecor, G.W. and Cochran, W.G. (1989): Statistical Methods, 8th ed., Iowa State University Press.

Steinmetz, K.L., Tyson, C.K, Meierhenry, E.F., Spalding, J.W, and Mirsalis, J.C. (1988): Examination of genotoxicity, toxicity and morphologic alterations in hepatocytes following *in vivo* or *in vitro* exposure to methapyrilene. Carcinogenesis, **9**, 959-963.

Turner, N.T., Woolley, J.L. Jr., Hozier, J.C., Sawyer, J.R. and Clive, D. (1987): Methapyrilene is a genotoxic carcinogen: Studies on methapyrilene and pyrilamine in the L5178Y/TK +/– mouse lymphoma assay. Mutat. Res., **189**, 285-297.

Urushidani, T. and Nagao, T. (2005): Toxicogenomics: The Japanese initiative. In Handbook of Toxicogenomics - Strategies and Applications. (Borlak, J., ed.), pp. 623-631. Wiley-VCH.

Waring, J.F., Ulrich, R.G., Flint, N., Morfitt, D., Kalkuhl, A., Staedtler, F., Lawton, M., Beekman, J.M. and Suter, L. (2004): Interlaboratory evaluation of rat hepatic gene expression changes induced by methapyrilene. Environ. Health Perspect., **112**, 439-448.

In Vitro Cell.Dev.Biol.—Animal
DOI 10.1007/s11626-007-9021-9

Chromosomal instability in human mesenchymal stem cells immortalized with human papilloma virus E6, E7, and hTERT genes

Masao Takeuchi · Kikuko Takeuchi · Arihiro Kohara · Motonobu Satoh · Setsuko Shioda · Yutaka Ozawa · Azusa Ohtani · Keiko Morita · Takashi Hirano · Masanori Terai · Akihiro Umezawa · Hiroshi Mizusawa

Received: 25 January 2007 / Accepted: 27 March 2007 / Editor: J. Denry Sato

Abstract Human mesenchymal stem cells (hMSCs) are expected to be an enormous potential source for future cell therapy, because of their self-renewing divisions and also because of their multiple-lineage differentiation. The finite lifespan of these cells, however, is a hurdle for clinical application. Recently, several hMSC lines have been established by immortalized human telomerase reverse transcriptase gene (hTERT) alone or with hTERT in combination with human papillomavirus type 16 E6/E7 genes (E6/E7) and human proto-oncogene, Bmi-1, but have not so much been characterized their karyotypic stability in detail during extended lifespan under in vitro conditions. In this report, the cells immortalized with the hTERT gene alone exhibited little change in karyotype, whereas the cells immortalized with E6/E7 plus hTERT genes or Bmi-1, E6 plus hTERT genes were unstable regarding chromosome numbers, which altered markedly during prolonged culture. Interestingly, one unique chromosomal alteration was the preferential loss of chromosome 13 in three cell lines, observed by fluorescence in situ hybridization (FISH) and comparative-genomic hybridization (CGH) analysis. The four cell lines all maintained the ability to differentiate into both osteogenic and adipogenic lineages, and two cell lines underwent neuroblastic differentiation. Thus, our results were able to provide a step forward toward fulfilling the need for a sufficient number of cells for new therapeutic

M. Takeuchi (✉) · K. Takeuchi · A. Kohara · S. Shioda · Y. Ozawa · A. Ohtani · H. Mizusawa
Division of Bioresources,
National Institute of Biomedical Innovation,
Osaka 567-0085, Japan
e-mail: takeuchim@nibio.go.jp

K. Takeuchi
e-mail: takeuchik@nibio.go.jp

A. Kohara
e-mail: kohara@nibio.go.jp

S. Shioda
e-mail: shioda@nibio.go.jp

Y. Ozawa
e-mail: ozaway@nibio.go.jp

A. Ohtani
e-mail: aohtani@nibio.go.jp

H. Mizusawa
e-mail: mizusawa@nibio.go.jp

M. Satoh
Health Science Research Resources Bank,
Osaka 590-0535, Japan
e-mail: satoh@osa.jhsf.or.jp

K. Morita · T. Hirano · A. Umezawa
National Research Institute for Child Health and Development,
Tokyo 157-8535, Japan

K. Morita
e-mail: morita-keiko@aist.go.jp

T. Hirano
e-mail: hirano-takashi@aist.go.jp

A. Umezawa
e-mail: umezawa@1985.jukuin.keio.ac.jp

M. Terai
Department of Reproductive Biology
and Pathology and Innovative Surgery,
National Research Institute for Child Health and Development,
Tokyo 157-8535, Japan
e-mail: terai@nch.go.jp

applications, and substantiate that these cell lines are a useful model for understanding the mechanisms of chromosomal instability and differentiation of hMSCs.

Keywords Human cord blood mesenchymal stem cell · Long-term culture · Karyotype analysis · mFISH CGH · Differentiation

Introduction

Tissue-specific stem cells in various adult tissues are known to be an important source in the regeneration of damaged tissue and maintenance of homeostasis in the tissues in which they reside. Among these stem cells, human mesenchymal stem cell (hMSC) has recently become of great interest in regenerative medicine, not only to replenish their own tissues, but also to give rise to more committed progenitor cells, which can differentiate into other tissues. MSCs in bone marrow have been shown to differentiate into several types of cell such as osteoblasts, adipocytes, chondrocytes, myocytes, and probably also neuronal cells (Okamoto et al. 2002; Takeda et al. 2004; Mori et al. 2005; Saito et al. 2005; Terai et al. 2005). Because of these properties, it is expected that hMSCs are an enormous potential source for future cell therapy. The goal of our study is to establish cell lines with long lifespan and with parental properties for clinical application. However, clinical application using these cells has been met with enormous difficulty, e.g., isolation of a cell population with specific criteria, expansion in vitro system for obtaining a sufficient number of cells without affecting their genomic characteristics and differentiation properties, and their storage in higher viability.

At present, there is a little evidence suggesting whether changes in these properties occur during expansion. Human normal MSCs have a limited capacity to replicate in the 40- to 50-population doubling level (PDL) at the most. To extend their lifespan, we have previously established human mesenchymal cell lines from human umbilical cord blood or bone marrow by immortalization with human telomerase reverse transcriptase (hTERT), human papillomavirus high-risk type 16 E6/E7 genes (HPV16E6/E7) or polycomb gene, Bmi-1 (Takeda et al. 2004; Mori et al. 2005; Terai et al. 2005).

hTERT-immortalization without affecting biological characteristics, despite extensive proliferation, has been reported in bone-marrow-derived hMSCs (Burns et al. 2005), human fibroblast (Milyavsky et al. 2003), and human keratinocyte (Harada et al. 2003), although it has been indicated that there is the possibility that prolonged culture of hTERT-immortalized fibroblasts may favor the appearance of clones carrying potentially malignant alterations (Milyavsky et al. 2003). HPV16, which encodes oncogenes (E6 and E7), can also immortalize hMSCs in vitro. Both E6 and E7 proteins act through their association with tumor suppressor gene products, p53 and retinoblastoma family members (pRb), respectively. E6 accelerates the degradation of the p53 protein, which is essential for cell arrest at the checkpoint in G_1/S and at the mitotic checkpoint when tetraploidy occurs (Cross et al. 1995), as well as at the G_2 phase under damaging conditions. E7 protein binds to pRb and abrogates the repressive function of these cell cycle regulations (Zheng et al. 2001). Thus, both p53 and pRb play a multitude of important roles in cell-cycle-progression checkpoints as reported in human keratinocytes (Patel et al. 2004), and fibroblasts (Khan et al. 1998). As a consequence, the disruption of the checkpoints that govern accurate cell division leads to abnormal segregation of chromosome and genomic instability, as shown in the cells immortalized with HPV16E6/E7 genes (Duensing et al. 2002).

In this paper, we report on the chromosomal instability and the differentiation activity during prolonged culture (cell expansion) using four mesenchymal stem cell lines. These results indicate that an umbilical cord blood-derived clone immortalized with hTERT (UCBTERT-21) showed normal karyotype for a period of 1 yr, whereas three other cell lines immortalized with HPV16E6/E7 and hTERT or HPV16E6, Bmi-1 and hTERT showed chromosomal instability but maintained the ability to differentiate.

Materials and Methods

Cell culture. Human mesenchymal stem cell lines, UCB TERT-21 (JCRB1107), UCB408E6E7TERT-33 (JCRB1110), UE6E7T-3 (JCRB1136), and UBE6T-6 (JCRB1140) were obtained from the JCRB Cell Bank (Osaka, Japan). Two of them are cell lines obtained by immortalizing human umbilical cord blood mesenchymal stem cells (UCB) with hTERT alone (UCBTERT-21; Terai et al. 2005) or with HPV16E6/E7 in combination with hTERT (UCB408E6E7TERT-33; Terai et al. 2005), and the two others are human bone-marrow-derived mesenchymal stem cell lines transformed with HPV16E6/E7 and hTERT genes (UE6E7T-3; Mori et al. 2005) or with bmi-1, HPV16E6 and hTERT genes (UBE6T-6; Takeda et al. 2004; Mori et al. 2005).

The UCBTERT-21 and UCB408E6E7TERT-33 were grown in PLUSOID-M medium (Med-Shirotori Co., Tokyo, Japan) or MSCGM BulletKit (Cambrex Co., East Rutherford, NJ). UE6E7T-3 and UBE6T-6 were cultured in POWEREDBY10 medium (Med-Shirotori Co.) or MSCGM BulletKit (Cambrex Co.); 5×10^3 cells/ml of each cell line were seeded and cultured for 7–10 d. When culture

plate was subconfluent, cells were treated with 0.25% trypsin/0.5 mM EDTA solution (both from Invitrogen, Tokyo, Japan) and replated at a density of 5×10^3 cells/mL.

All of the cells were maintained in a humidified incubator at 37° C and 5% CO_2. PDLs were calculated using the formula: PDL= log (cell output/input)/log2. At the starting cultivation, PDLs of UCBTERT-21, UCB408E6E7 TERT-33, UE6E7T-3, and UBE6T-6 were 42, 67, 60, and 56, respectively. The doubling time of the UCB408E6E7T-33 cell was 1.5 d, and that of UCBTERT-21, UE6E7T-3, or UBE6T-6 was 2.6, 2.0, or 4.0 days, respectively.

Measurement of chromosome number and fluorescence in situ hybridization. Metaphase chromosome spreads for measurement of chromosome number and fluorescence in situ hybridization (FISH) were prepared from exponential growing cells at various PDL. The cells were treated in a hypotonic solution after exposure to 0.06 μg/ml colcemid (Invitrogen, Carlsbad, CA) for 2 h and fixed in methanol/acetic acid (3:1). The cells were spread on a microscope slide.

To count the number of chromosomes, the cells were stained with DAPI (4'-6-diaminido-2-phenylindol; Vector Laboratories, Inc. Burlingame, CA) and examined under an Axioplan II imaging microscope (Carl Zeiss, GmbH) equipped with Leica QFISH software (Leica Microsystems Holding, UK). To examine statistically significant chromosome numbers, we have allowed ±1 deviation and 50–100 metaphase spreads were scored for each assay.

Painting probes specific for chromosome 13 (XCP13-kit; FITC; MetaSystems, GmbH) and chromosome 17 (XCP17-kit; Texas Red) (MetaSystems GmbH, Altlussheim, Germany), and multicolor probes (mFISH-24Xcyte-kit, DAPI, FITC, TexasRed, Cy3, Cy5, and DEAC; MetaSystems GmbH) were used for FISH analysis. FISH was performed according to the manufacture's protocol (MetaSystems GmbH). Briefly, both the metaphase chromosome spread and the probe were denatured with 0.07 N NaOH or 70% formamide, hybridized at 37° C for 1–4 d, and counterstained with DAPI. FISH images were captured and analyzed on the Zeiss Axio Imaging microscope (Carl Zeiss Microimaging GmbH, Jena, Germany) with Isis mBAND/mFISH imaging Software (MetaSystems GmbH).

CGH analysis. Hybridization was carried out with the BAC Array (MAC ArrayTM Karyo 4000 Component, Macrogen Co., Rockville, MD) by the Hybstation (Genomic Solutions, Ann Arbor, MI). Briefly, test DNAs, which were isolated using an isolation kit (Amersham BioSciences, Little Chalfont, UK) and Spin Column (QIAGEN Co., Tokyo, Japan), and reference DNAs (Promega Co., Madison, WI), were labeled, respectively, with Cy3 or Cy5 (BioPrimer DNA Labeling System, Invitrogen Co.), precipitated together with ethanol in the presence of Cot-1 DNA, redissolved in a hybridization mixture (50% formamide, 10% dextran sulfate, 2xSSC, 4% sodium dodecyl sulfate [SDS], pH 7), and denatured at 75° C for 10 min. After incubation at 37° C for 30 min, each mixture was applied to an array slide and incubated at 42° C for 48–72 h. After hybridization, the slides were washed in a solution of 50% formamide—2× SSC (pH 7.0) for 15 min at 50° C, in 2× SSC—0.1% SDS for 15 min at 50° C, and in a 100-mM sodium phosphate buffer containing 0.1% Nonidet P-40 (pH 8) for 15 min at room temperature, then scanned with GenePix4000A (Axon Instruments, Union City, CA). Acquired images were analyzed with MacViewer (Macrogen Instruments).

Differentiation ability. To evaluate the differentiation potential of each cell line, cells were cultured on a coverslip in each induction medium, that is, hMSC Differentiation BulletKit-Adipogenic (PT-3004, Cambrex BioScience, Inc., Walkersville, MD) for adipocyte and NPMM Bullet kit (NPMM™ BulletKit (B3209, Cambrex BioScience) for neural progenitor cells. For osteoblast, cells were treated with 0.1 μM dexamethasone (Sigma Chemical Co., St. Louis, MO), 50 μg/ml L-ascorbic acid (Sigma Chemical), and 10 mM β-glycerophosphate (Sigma Chemical) in the PLUSOID-M medium (Med-Shirotori Co.) or the POWER-EDBY10 medium (Med-Shirotori Co.) of culture medium.

After 2–4 wk, the cells were washed in phosphate-buffered saline (PBS), fixed in 4% paraformaldehyde in PBS and stained with Oil Red-O (Sigma Chemical) for detection of adipocyte, and with alkaline phosphatase staining solution containing 0.25 mg/ml naphthol AS-BI phosphate and 0.25 mg/ml Fast violet LB salt for detection of alkaline phosphatase-positive osteoblast. In immunostaining for neuron-like cells, the cells fixed with paraformaldehyde were permeabilized with methanol at −20° C for 10 min and stained with an anti-IIIβ tubulin antibody (Sigma Chemical) or anti-neurofilament antibody NF-200 (Sigma Chemical) and Texas Red-anti-mouse IgG (Southern Biotechnology Associates, Inc., Birmingham, AL) as previously described (Takeuchi et al. 1990).

Results

Changes in chromosomal number in human mesenchymal stem cell lines in prolonged culture. Immortalization of cultured cells frequently induces an abnormal chromosome number as shown in cancer cells (Duensing et al. 2000; Munger et al. 2004; Patel et al. 2004), especially at higher frequency in long-term culture. We therefore examined four cell lines, human mesenchymal stem cell (hMSC) lines immortalized with combinations of bmi-1, E6, E7, and/or hTERT genes, for chromosome instability by counting metaphase chromosomes.

All of the lines were diploid, each containing 46 up to 40 PDL including the PDL numbers of nontransfecting original MSCs (Takeda et al. 2004; Mori et al. 2005; Terai et al. 2005). For UCBTERT-21 cell, no further changes in chromosome number have been observed up to date (for PDL 133) as shown in Fig. 1*A* and *B*. In contrast, although the UBE6T-6 cell and the UE6E7T-3 cell were near diploid, both cells exhibited considerable variation in chromosome number from PDL 70 after the culture started. For example, when the assay of UE6E7T-3 cells start at PDL 62 in culture, 90% of cell population had 46 chromosomes, but the population decreased with prolonged culturing and a population containing 44 chromosomes became dominant (43% of cell populations) at PDL 147 (Fig. 1*E*, *F*). A similar variation was also observed in UBE6T-6 cells (Fig. 1*C*, *D*).

To ascertain whether or not the changes observed were induced by transfection with HPV16E6E7, we assayed the chromosome numbers of UCB408E6E7TERT-33 cell in prolonged culture. The cell line showed similar chromosomal changes to those of the UE6E7T-3 cell, the rate of which was more rapid. At day 2 after culture by us changes became evident (PDL 68), the UCB408E6E7TERT-33 cells consisted of two distinct populations concerning chromosome number (near diploid [24%] and near tetraploid [53%]), shown in Fig. 1*G*. However, the near diploid population was unstable and decreased gradually. At PDL 81, the population became only near tetraploid, 80% of the

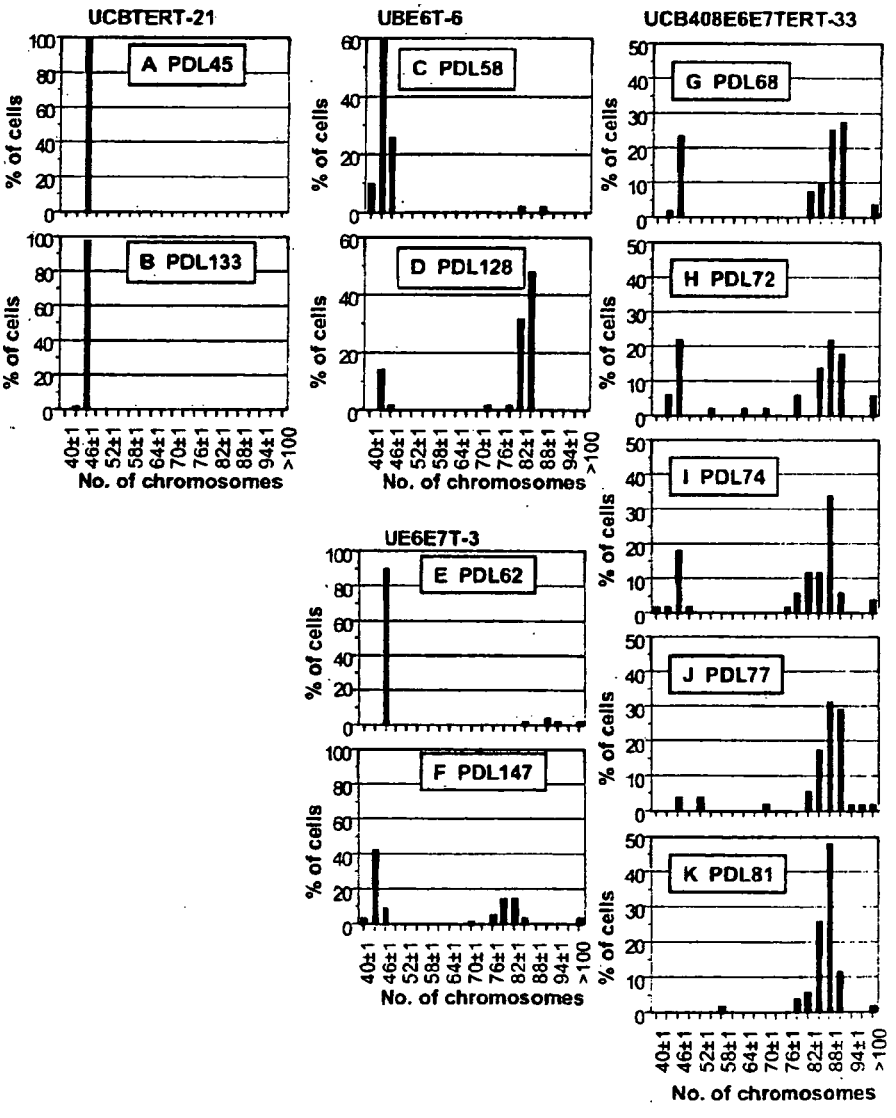

Figure 1. Changes in chromosomal numbers in prolonged cultures of four hMSC cell lines. (*A*-*K*) The chromosomal numbers at various culture stages were counted by DAPI staining. (*A*, *B*), (*C*, *D*), (*E*, *F*), and (*G*-*K*) represent the chromosomal numbers from UCBTERT-21, UBE6T-6, UE6E7T-3; and UCB408E6E7TERT-33, respectively. To examine statistically significant chromosomal numbers, we have allowed ±1 deviation, and 50-100 metaphase spreads were examined for each assay. *Note* the changes in chromosomal number from near 2*n* to near 4*n* in prolonged culture.

cells contain 85–92 chromosomes (Fig. 1*K*). The results indicate that UCBTERT-21 is relatively stable in chromosome number, whereas each of the oncogene-immortalized cells (UE6E7T-3, UBE6T-6, and UCB408E6E7TERT-33 cell) were unstable in chromosome numbers, which altered substantially during prolonged culture.

We next applied FISH and CGH analysis to characterize the chromosomal aberrations of the cell lines. All of the four cell lines passed for PDL 50 before examination by FISH. mFISH analysis of the UCBTERT-21 cell at PDL 52 showed normal chromosome composition (Fig. 2*A* and *B*) as observed in non-immortalized cells. The UBE6T-6 cell containing 43–45 chromosomes demonstrates losses of chromosome 13, 16, and 19 (marginal variation in chromosome 4 was observed among cells), but keeps on proliferating in chromosome number of 43–45 (Fig. 2*D*, *E*). In contrast, the UCB408E6E7TERT-33 cell showed more heterogeneity in chromosome composition with intrachromosomal and interchromosomal aberrations (data not shown). However, by mFISH analysis we were able to detect nonrandom losses of chromosome 13 in three cell lines except the UCBTERT-21 cell line. This was also confirmed by pFISH analysis using the probes specific for chromosome 13 and chromosome 17 (Fig. 2*C*, *F*). More than 97% of UCBTERT-21 cells showed two copies for chromosome 13, indicating the stability of the chromosomes in the cell line (Fig. 2*G*). The UE6E7T-3 and the UBE6T-6 cell lines with chromosome numbers of 43 45 showed only one copy of chromosome 13 in 76% of UE6E7T-3 cells and 86% of UBE6T-6 cells, respectively (Fig. 2*I*, *J*). A similar loss of chromosome 13 was also observed in 70% of UCB408E6E7TERT-33 cells, which showed three copies of chromosome 13 in near tetraploid (Fig. 2*H*). Other chromosomes, for example chromosome 17, were contained in the UCBTERT-21 and UBE6T-6 cell lines (Fig. 2*C*, *F*).

Furthermore, a significant nonrandom loss of chromosome 13 at the single cell-level observed by FISH was examined by array CGH, which samples the entire cell population. Figure 3 shows the array CGH profiles from early (*blue spots*) and late (*red spots*) stages of proliferating of each cell line. The UCBTERT-21 cell did not show any detectable differences in array CGH profiles between early and late stages (Fig. 3*A*). Although the loss of chromosome 13 had already occurred at early stages in the UBE6T-6 and the UCB408E6E7TERT-33 cell lines, in addition to the losses of chromosomes 4, 9, and 16 (Fig. 3*B*, *D*), in UE6E7T-3 the loss appeared between PDL 78 to 101 with loss of chromosome 16. The most compelling observation was that all three cell lines revealed a consistent whole loss of chromosome 13. These data are consistent with the results observed by FISH analysis. From these results, we

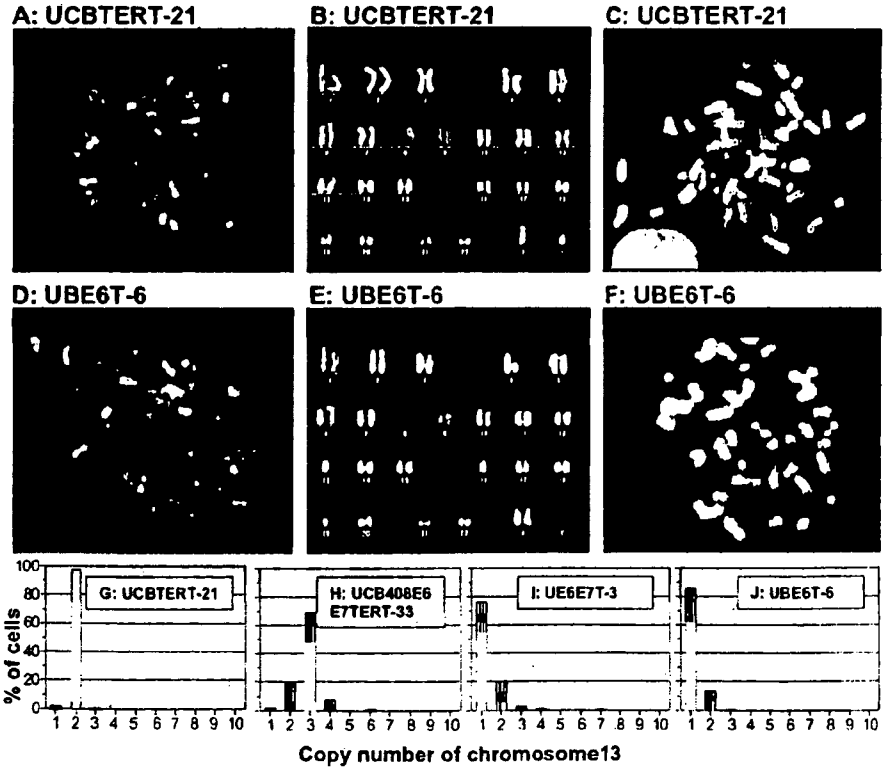

Figure 2. FISH analysis of human mesenchymal stem cell (hMSC) lines immortalized with hTERT alone, hTERT plus bm-1, HPVE6 or with hTERT plus HPVE6/E7. Multicolor FISH images of metaphase spreads (*A*, *D*), their karyotypes (*B*, *E*), and painting FISH images using DNA probes specific for chromosome 13 (*green*) and 17 (*red*) (*C*, *F*) of UCBTERT-21 (*A*, *B*, *C*) and UBE6T-6 (*D*, *E*, *F*). Quantity of chromosome 13 copy numbers in four cell lines (*G–J*). FISH signals were counted in 120~200 metaphase spreads plus interphase nuclei. UCBTERT-21 cells contained two copies of chromosome 13 and 17, and showed normal human karyotype, whereas other cells lost one copy of chromosome 13.

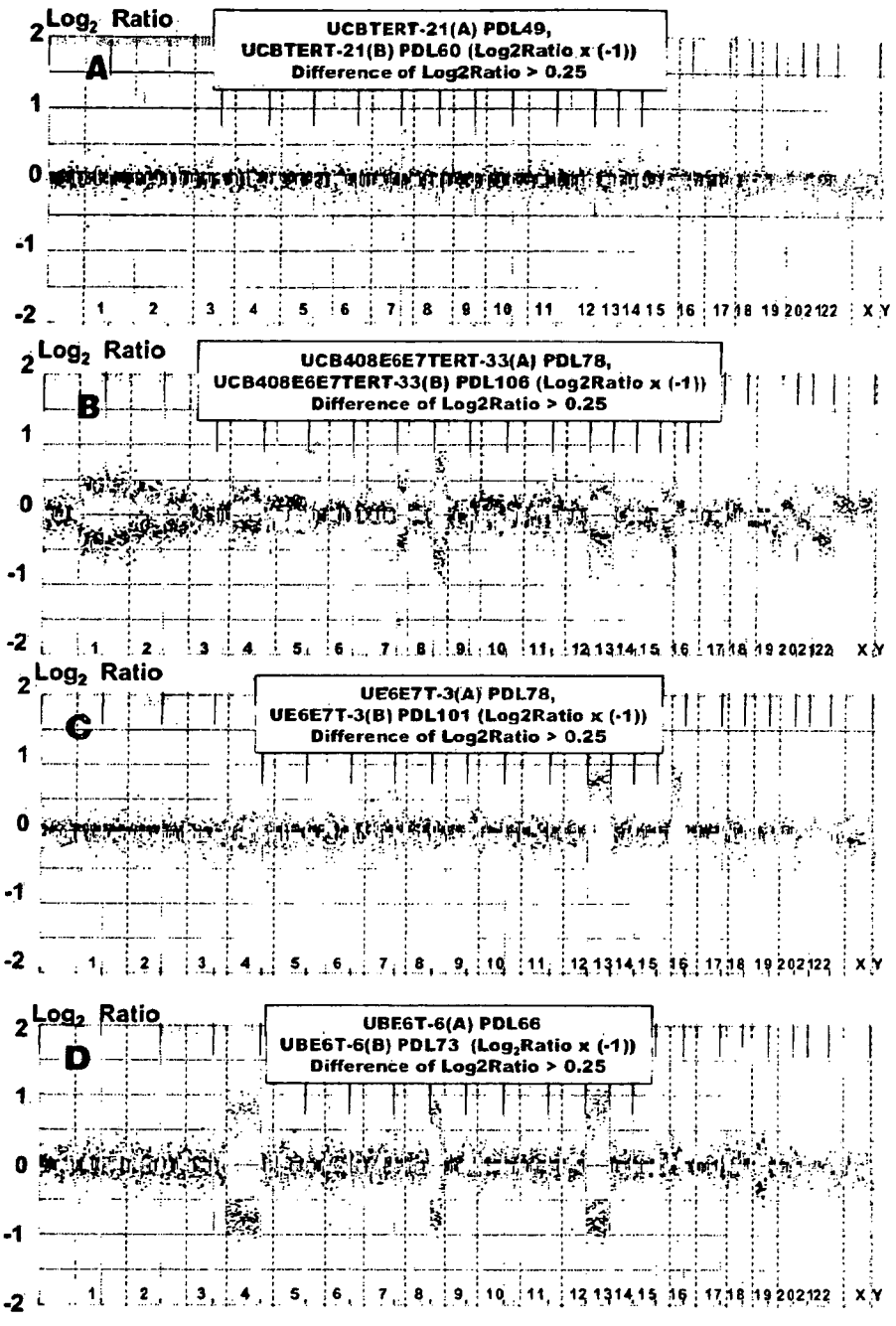

Figure 3. Array CGH profiles performed on four immortalized human mesenchymal stem cell lines at selected PDL. For each *panel*, the *X*-axis represents the 22 autosomes, the *X* and *Y* chromosomes, and the *Y*-axis shows the $\log_2$ of the fluorescence intensity ratio (cy3 [hMSCs]/cy5 [normal cell]) of all spots of the chromosome. Values above 0 (*red spots*) or values below 0 (*blue spots*) signify a loss of chromosome (chromosome regions). *Blue spots* in each *panel* indicate the $\log_2$ ratios observed at early stage in the culture of each cell line, which are overlaid with *red spots* indicated at the late stage. *Green spots* indicate the difference in value between *blue spots* and *red spot*. *Note* that in the UE6E7T-3 cell line, one copy of chromosome 13 and 16 were lost between PDL 78 and 101.

concluded that only hTERT-mediated immortalization induced little change in the chromosome numbers and chromosome structures of mesenchymal stem cells, but immortalization with Bmi-1, E6, and E7 in addition to hTERT results in chromosome instability.

Differentiation potential into lineages of immortalized mesenchymal stem cell lines. It has been reported that mesenchymal stem cells have the extensive potential to differentiate into multiple cell lineages including osteoblast, chondrocytes, adipocytes (Pittenger et al. 1999), cardiac myocytes (Makino et al. 1999), and neural cells (Pacary et al. 2006; Wislet-Gendebien et al. 2005). To evaluate whether chromosome instability of these cell lines in prolonged culture affects differentiation, cells of each cell line were stimulated in each induction medium for 2 to 4 wk. In